

PHASE-CHANGE SOLVENTS FOR THE CAPTURE AND RELEASE OF CO₂
AND
CO₂-SOLUBLE SURFACTANTS FOR STABILIZATION OF CO₂-IN-BRINE FOAMS

by

Bing Wei

B.S. in Chemical Engineering, Dalian University of Technology, 2008

Submitted to the Graduate Faculty of
Swanson School of Engineering in partial fulfillment
of the requirements for the degree of
Master of Science

University of Pittsburgh

2010

UNIVERSITY OF PITTSBURGH
SWANSON SCHOOL OF ENGINEERING

This thesis was presented

by

Bing Wei

It was defended on

November 22, 2010

and approved by

Yee Soong, Acting Division Director

National Energy Technology Laboratory

Sachin Velankar, Associate Professor

Department of Chemical and Petroleum Engineering

J. Karl Johnson, Professor

Department of Chemical and Petroleum Engineering

Robert M. Enick, Professor

Department of Chemical and Petroleum Engineering

Thesis Advisor

Copyright © by Bing Wei

2010

PHASE-CHANGE SOLVENTS FOR THE CAPTURE AND RELEASE OF CO₂
AND
CO₂-SOLUBLE SURFACTANTS FOR STABILIZATION OF CO₂-IN-BRINE FOAMS

Bing Wei, M.S.

University of Pittsburgh, 2010

The first intention of this research is to identify specific CO₂-philic solids from two candidates, namely sugar acetates and tert-butylated aromatics, which can be used to separate high pressure CO₂ from H₂. In this work, many of these solids were found to melt in the presence of high pressure CO₂ (600 – 1000 psi) and absorb large amounts of CO₂. It was hoped that upon exposure to a 1:1 CO₂/H₂ high pressure gas mixture that was selected to be representative of a shifted gasifier effluent stream, the solid would melt and selectively absorb CO₂. Only one candidate, glucose pentaacetate, was found to melt in the presence of the gas mixture at 25 °C. The pressure of the system was ~6000 psi, which is unrealistically high for the commercial application of this process. Therefore mixed gas solubilities in the molten phase were not determined.

In a second project, a strategy for using CO₂-soluble compounds to decrease the mobility of dense CO₂ in porous media was investigated. It is to inject a CO₂ surfactant solution into the porous media, which contains both brine and oil, thereby generating a low mobility emulsion or foam of CO₂ droplets separated by surfactant-stabilized brine lamellae that bridge pore throats. In this work, the surfactants were screened by assessing their ability to stabilize foams when

equal volumes of CO₂ and brine were mixed with the amount of surfactant capable of dissolving in the CO₂ at test conditions (e.g. 25 °C and 1300 psi). Stability was assessed by monitoring the rate of collapse of the foam and the appearance of clear zones of excess water and CO₂.

We have established the identity of several non-ionic, hydrocarbon-based, commercially available, inexpensive surfactants that can dissolve in CO₂ at typical EOR reservoirs conditions to a high enough concentration (~0.02-0.20 wt%) to form relatively stable emulsions/foams of liquid or supercritical CO₂ droplets separated by films of brine. Although these surfactants are CO₂-soluble, they are even more water-soluble, therefore they tend to partition into the low-volume brine phase and stabilize the emulsion form emulsions in which the brine is the low-volume (e.g. 10 vol%) continuous phase, in accordance with Bancroft's rule. The most effective thickeners were branched alkyl phenol ethoxylates, linear alkyl phenol ethoxylates, and linear alkyl ethoxylates. Linear ethoxylated alcohols was ineffective foam stabilizers.

TABLE OF CONTENTS

1.0	INTRODUCTION.....	1
1.1	OBJECTIVES.....	2
1.2	INTEGRATED GASIFICATION COMBINED CYCLE (IGCC)	3
1.3	CO ₂ -PHILIC SOLIDS	4
2.0	PRELIMINARY WORKS AND RESULTS	7
2.1	VERIFICARION OF THE GAS COMPOSITION.....	7
2.2	EXPERIMENT APPARATUS.....	8
2.3	PURIFICATION OF SAMPLES	9
2.4	PURITY ANALYSIS OF SAMPLES	10
2.5	CO ₂ PHASE BEHAVIOR OF THE SOLID ABSORBENTS.....	12
3.0	INTRODUCTION.....	16
3.1	REDUCING MOBILITY OF CO ₂ IN POROUS MEDIA.....	17
3.1.1	DIRECT THICKENERS.....	18
3.1.2	WAG RELATIVE PERMEABILITY REDUCTION	19
3.1.3	SAG RELATIVE PERMEABILITY REDUCTION	19
3.2	SURFACTANTS DESIGN GUIDELINES	20
4.0	PRELIMINARY WORK AND RESULTS.....	22
4.1	EXPERIMENT APPARATUS	22

4.2	SOLUBILITY AND FOAM STABILITY TESTS	23
4.2.1	BRANCHED ALKYLPHENOL ETHOXYLATES.....	25
4.2.2	LINEAR ALKYLPHENOL ETHOXYLATES-STEPAN NONYLPHENOL CEDEPAL CO 630 AND 710.....	35
4.2.3	BRANCHED ALKYL ETHOXYLATE.....	37
4.2.4	MONOLAURATE POLYETHYLENEGLYCOL	43
4.2.5	LINEAR ALKYL ETHOXYLATES/BRIJ SURFACTANTS	44
4.3	SACROC BRINE FOAM TESTING.....	47
5.0	SUMMARY.....	51
APPENDIX A	53
	VAPOR-LIQUID EQUILIBRIUM FOR H ₂ +CO ₂ SYSTEM.....	53
BIBLIOGRAPHY	57

LIST OF TABLES

Table 1. Proposed CO ₂ -philic solids for the selective separation of CO ₂ from H ₂	4
--	---

LIST OF FIGURES

Figure 1. Illustration of IGCC power plant.....	4
Figure 2. Comparison of dew point data from literature and experiment.....	7
Figure 3. Diagram of high pressure, variable-volume, windowed cell.....	9
Figure 4. DSC of the unpurified TTBP.....	11
Figure 5. DSC of the purified TTBP.....	11
Figure 6. Pressure-composition diagram for glucose pentaacetate and H ₂ -CO ₂ system at 300 K.....	13
Figure 7. Pressure-composition diagram for β-D-Ribofuranose 1,2,3,5-tetraacetate at 298 K.	14
Figure 8. Pressure-composition diagram for Sucrose octaacetate at 298 K.	14
Figure 9. Pressure-composition diagram for 2-6-Di-tert- butyl-4-methylphenol at 298.15 K	15
Figure 10. Structure of PolyFAST	18
Figure 11. Foam stability test cartoon description	23
Figure 12.DOW Triton X 100, BASF Lutensol OP 10 and Huntsman octylphenol Surfonic 100 and 120	25
Figure 13.Solubility of Dow Triton X 100, BASF Lutensol OP 10 and Huntsman octylphenol Surfonic OP 100 and 120 in CO ₂ at 25 °C.	26
Figure 14. 0.04wt% Triton X-100 and 0.03% BASF OP 10 in CO ₂ at 1300 psi and 25 °C , with a brine (5 wt% NaCl) / CO ₂ volume ratio 1:1	26
Figure 15. DOW Tergitol NP Series, n = 4-15	28

Figure 16. The effect of the average number of EO groups on the solubility of Tergitol NP series of branched, nonylphenol ethoxylates in CO ₂ at 25 °C and 58 °C.....	28
Figure 17. Foam stability associated with the Dow Tergitol NP series foams at 1300 psi and 25 °C, with a brine (5 wt% NaCl) /CO ₂ volume ratio 50:50.....	30
Figure 18. Huntsman Surfonic N 85, 100, 120, 150, 200, x = 8.5, 10, 12, 15, 20.....	31
Figure 19. The effect of the average number of EO groups on the solubility of Huntsman N series of branched, nonylphenol ethoxylates in CO ₂ at 25 °C and 58 °C.....	31
Figure 20. Huntsman Surfonic N series foams at 1300 psi and 25°C with a brine (5 wt% NaCl)/CO ₂ volume ratio 50:50; 0.04 wt% N 85, 0.03% N120 and N150.....	32
Figure 21. Huntsman Surfonic DDP 100 and 120, x = 10, 12.....	33
Figure 22. The solubility of Huntsman Surfonic DDP 100 and 120 branched, mixed isomeric, dodecylphenol ethoxylate in CO ₂ at 25 °C	33
Figure 23. Stepan Cedepal CO 630 and 710, x = 10, 10.5.....	35
Figure 24. Solubility of Stepan CO 630 and 710 in CO ₂ at 25 °C.....	35
Figure 25. 0.03wt% Stepan CO 710 and CO 630 in CO ₂ at 1300 psi and 25 °C, with a brine (5 wt% NaCl)/CO ₂ volume ratio 50:50	36
Figure 26. DOW Tergitol TMN Series, x = 6.....	37
Figure 27. DOW Tergitol TMN 6 branched trimethylnonyl ethoxylate (10% water) in CO ₂ at 25°C and 60 °C.....	37
Figure 28. BASF Lutensol XP 70 and 80, x=7 and 8 (C ₁₀ alkyl chain structure is proprietary) ..	38
Figure 29. The solubility of BASF XP 70 and XP 80 in CO ₂ at 25 °C and 60 °C.....	39
Figure 30. Foam stability of 0.04wt% BASF XP 70 in CO ₂ at 1300 psi and 25 °C, with a brine (5wt% NaCl)/ CO ₂ volume ratio 1:1.....	40
Figure 31. Huntsman isotridecyl ethoxylate TDA 8 and 9, x = 8 and 9, Huntsman are branched C ₁₃ alcohol ethoxylates.	41
Figure 32. BASF Lutensol TO 8 and 10 and Huntsman TDA 8 and 9 in CO ₂ at 25 °C.....	41
Figure 33. Foam stability of 0.03wt% BASF TO 8, 10, and Huntsman TDA 8 in CO ₂ at 1300 psi and 25 °C, with a brine (5 wt% NaCl)/CO ₂ volume ratio 1:1	42

Figure 34. Huntsman Empilan KR 6 and 8, the 6- and 8-mole ethoxylate of an α -methyl primary C ₉₋₁₁ alcohol	42
Figure 35. Huntsman Empilan KR 6 and 8.....	43
Figure 36. Sigma Aldrich PEG monolaurate 600, x = 9	43
Figure 37. Solubility of monolaurate PEG in CO ₂ at 25 °C.	44
Figure 38. Huntsman L12-6 and 12-8, the six-mole and eight-mole ethoxylates of linear, primary C ₁₀₋₁₂ alcohol, Brij surfactants C ₁₁ E ₆ and C ₁₁ E ₈ .Sigma Aldrich decaethyleneglycol monododecylether, Brij surfactant C ₁₂ E ₁₀	44
Figure 39. Huntsman L12-8 and L12-6 in CO ₂ at 25 °C	45
Figure 40. Sigma Aldrich decaethyleneglycol monododecylether	45
Figure 41. Foam stability of 0.2% Dow NP 15, 0.2% Huntsman N 120, and 0.2 wt% Huntsman N 150 in CO ₂ at 3200 psi and 58 °C, with SACROC brine volume ratio 1:1	48
Figure 42. Foam stability of 0.05 wt% Huntsman N 200 in CO ₂ at 3150 psi and 71.1 °C, with West Hastings brine (111000ppm) volume ratio 1:1	49
Figure 43. Foam stability of 0.05 wt% Huntsman N 150 or 200 in CO ₂ at 2100 psi and 57.2 °C, with Delhi brine (78000ppm) volume ratio 1:1	49
Figure 44. Foam stability of 0.05 wt% Huntsman N 200 in CO ₂ at 2600 psi and 73.3 °C, with Woodruff brine (129000ppm) volume ratio 1:1	50
Figure 45. Foam stability of Huntsman N 200 in CO ₂ at 2750 psi and 66.7 °C, with Eutaw brine (90000ppm) volume ratio 1:1	50
Figure A1. Vapor-liquid equilibrium for H ₂ +CO ₂ binary system at 280 K, ▲x:mole fraction of H ₂ in liquid phase, ◆y:mole fraction of H ₂ in gas phase.....	53
Figure A2. Vapor-liquid equilibrium for H ₂ +CO ₂ binary system at 278.15 K, ▲x:mole fraction of H ₂ in liquid phase, ◆y:mole fraction of H ₂ in gas phase.....	54
Figure A3. Vapor-liquid equilibrium for H ₂ +CO ₂ binary system at 259.9 K, ▲x:mole fraction of H ₂ in liquid phase, ◆y:mole fraction of H ₂ in gas phase.....	54
Figure A4. Vapor-liquid equilibrium for H ₂ +CO ₂ binary system at 250 K, ▲x:mole fraction of H ₂ in liquid phase, ◆y:mole fraction of H ₂ in gas phase.....	55
Figure A5. Vapor-liquid equilibrium for H ₂ +CO ₂ binary system at 244.9 K, ▲x:mole fraction of H ₂ in liquid phase, ◆y:mole fraction of H ₂ in gas phase.....	55

Figure A6. Vapor-liquid equilibrium for H_2+CO_2 binary system at 229.9 K, ▲x:mole fraction of H_2 in liquid phase, ◆y:mole fraction of H_2 in gas phase.....56

Figure A7. Vapor-liquid equilibrium for H_2+CO_2 binary system at 219.9 K, ▲x:mole fraction of H_2 in liquid phase, ◆y:mole fraction of H_2 in gas phase.....56

1.0 INTRODUCTION

The greenhouse effect is the rise in earth temperature caused by certain gases in the atmosphere like CO₂, CH₄, and water vapor that absorb and emit radiation within the thermal infrared range. The trapping of the excessive greenhouse gases leads to more heating and a higher resultant earth temperature, and may trigger disastrous consequences such as loss of snow cover, sea level rise, and a change in weather patterns. A worldwide report shows that CO₂ emissions from human activities have increased from an insignificant level two centuries ago to annual emissions of more than 33 billion tons today [1]. Also, the most recent report from the Nobel Prize-winning Intergovernmental Panel on Climate Change (IPCC) concluded that global CO₂ emissions must be cut by 50-80% by 2050 if the most damaging effects of global warming are to be avoided. CO₂ capture and storage (CCS) is a set of technologies intended to solve this global issue by capturing CO₂ emitted from industrial and energy-related sources before it enters the atmosphere. Thus our challenge primarily lies in the aspect of how to produce energy in a low-carbon, cost-effective and environmentally friendly manner to sustain a long term industrial-scale energy generation. CO₂ generated as a by-product from industrial processes such as integrated gasification combined cycle (IGCC), synthetic ammonia production, and H₂ production can be captured or reused by the current existing capture techniques or proposed novel technologies including absorption, adsorption, low-temperature distillation, gas separation

membranes and mineralization and biomineralization. The aim of this project is to identify specific CO₂-philic solids from two types of candidates, sugar acetates and tert-butylated aromatics, which can be used to separate CO₂ from H₂ found in a high pressure stream and then potentially release the CO₂ with a very modest pressure drop during regeneration.

1.1 OBJECTIVES

Tert-butylated aromatics and sugar acetates melt in the presence of high pressure CO₂ at ambient temperature and absorb large amounts of CO₂. The CO₂/H₂ binary was chosen for assessing the ability of these solids to selectively absorb CO₂ because several industrial processes such as integrated gasification combined cycle (IGCC) produce this mixture of gases.

Before this research, several CO₂-philic solids phase behavior with CO₂ have been tested in Dr. Enick's lab at the University of Pittsburgh [1]. The sugar acetates are thought to be quite CO₂-philic because of the Lewis acid : Lewis base interactions between the sugar acetates and CO₂ at high pressures. The reason that tert-butylated aromatics are CO₂-philic is not as obvious, although it may be associated with the low cohesive energy density of the t-butyl groups. In this research, we will determine the phase behavior of CO₂ with the solids, H₂ with the solids, and then the phase behavior of CO₂/H₂ and CO₂-philic solids in an attempt to identify the temperature and pressure conditions at which CO₂-based capturing (i.e. conditions required for the solids to melt in the presence of the binary gas mixture) may be effective. A H₂ and CO₂ at the molar ratio of 1:1 was chosen because flue gas from coal-fired power plants contains 10-12 percent CO₂ by volume, which is almost the same as H₂[2]. The performance of the CO₂-philic solids will be tested in terms of cloud point pressure and freezing point pressure. Before

experiments, the composition of the gas mixture has to be verified and the CO₂-philic solids have to be purified to make sure the experiment result is accurate, and the specific method will be discussed in detail later. Also, the phase behavior of CO₂+solid and H₂+solid will be tested separately to study the solubility of each gas before we study the phase behavior of the CO₂+H₂+solid system.

1.2 INTEGRATED GASIFICATION COMBINED CYCLE (IGCC)

As an emerging coal-based technology for electric power generation, IGCC is gaining attention as a potentially attractive option to lessen emissions of CO₂ and conventional air pollutants. In IGCC technology, coal is converted into a high value syngas of CO and H₂ and then the gases react with steam and undergo the water gas shift (WGS) reaction to form CO₂ and H₂ [3]. The CO₂ in these exhaust gases must be separated and concentrated before it is diluted in the combustion stage. After cleanup H₂ is used as primary fuel for the combined cycle's gas turbine. CO₂-philic absorbents could be used as an essential part of the IGCC to convert coal into hydrogen fuel while capturing CO₂ for sequestration[4].

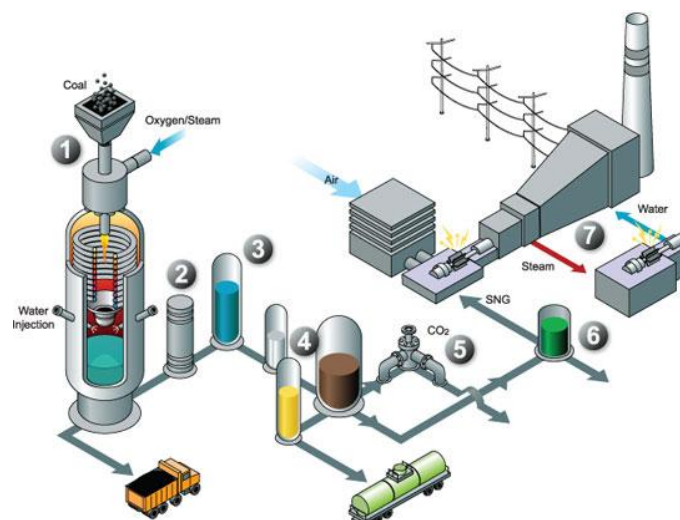


Figure 1. Illustration of IGCC power plant

1.3 CO₂-PHILIC SOLIDS

Two classes of CO₂-philic solids are chosen: tert-butylated aromatics and sugar acetates.

The chemical structure for each compound is listed in [Table 1](#).

Table 1. Proposed CO₂-philic solids for the selective separation of CO₂ from H₂

Compounds	Structure
2,4,6-tri-tert-butylphenol	

Table 1 (continued)

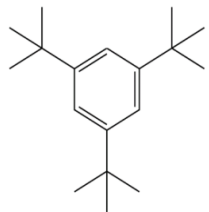
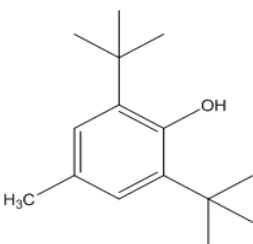
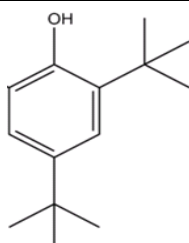
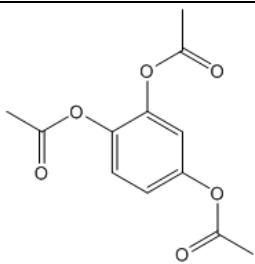
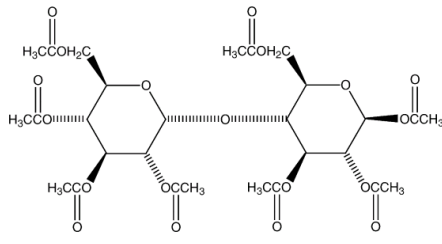
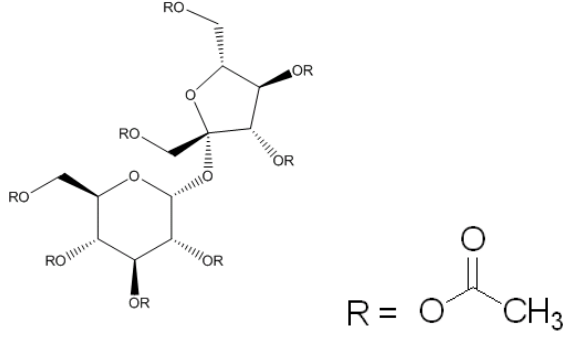
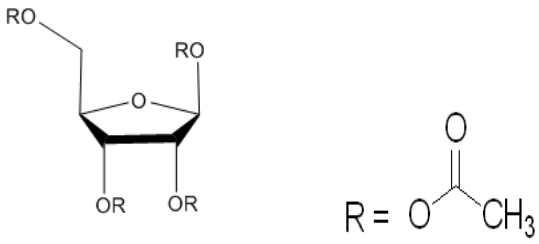
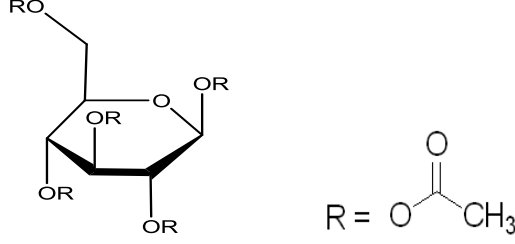
1,3,5- tri-tert-butylbenzene	
2-6-di-tert- butyl-4-methylphenol	
2,4-di-tert-butylphenol	
1,2,4-tri-acetoxybenzene	

Table 1 (continued)

<p>β-D-maltose octaacetate</p>	
<p>D-(+)-sucrose octaacetate</p>	
<p>β-D-ribofuranose 1,2,3,5-tetraacetate</p>	
<p>β-D-glucose pentaacetate</p>	

2.0 PRELIMINARY WORKS AND RESULTS

2.1 VERIFICARION OF THE GAS COMPOSITION

A cylinder of analyzed gas mixtures CO₂-H₂ (50%-50%) was supplied by Valley National Company. Verification of this composition was performed by conducting isothermal compression and expansions of this gas sample. Dew point data were collected and compared with the previously published vapor-liquid equilibrium data ([Appendix A](#)) for this particular mixture in the temperature range of 220K to 298.15K and the pressure range of 200 psi to 2400 psi. [\[5\]\[6\]\[7\]](#) The results, shown in the following figure, confirm that the cylinder is an equimolar mixture of CO₂ and H₂.

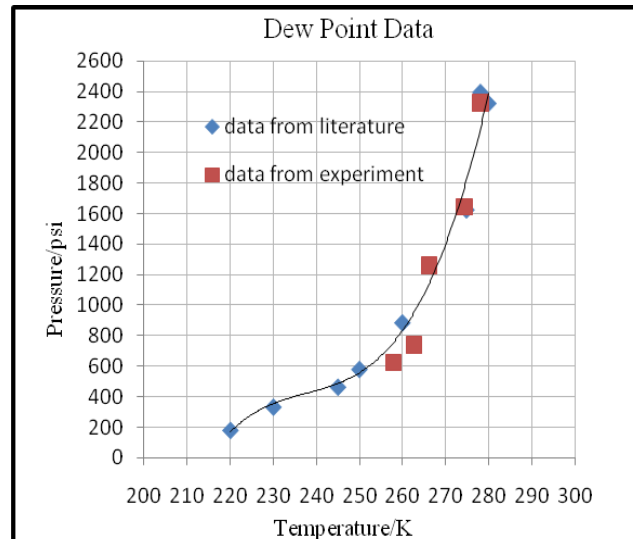


Figure 2. Comparison of dew point data from literature and experiment

2.2 EXPERIMENT APPARATUS

The vapor-liquid equilibrium experiment of gas mixtures were performed at five different temperatures using a high pressure, variable-volume, windowed cell (D. B. Robinson Cell), with a cylindrical sample volume, as shown in [Figure 3](#). Isothermal compression and expansions of gas mixture is used to determine the dew point data. The procedure is as follows. First, the overburden silicone oil was injected into the cell and directly flowed into the space surrounding the quartz tube and into the bottom of the quartz tube beneath the floating piston, then the gas mixture was added into the sample chamber and the inlet valve is closed to isolate the sample volume from the high pressure gases in the pump. The pressure of the sample volume can be increased by pumping the overburden oil into the windowed cell. The pressure of the sample volume is increased by compressing the sample volume. The overburden oil was injected at a low flow rate until visual observation of a mist of a liquid phase appeared in the sample volume. Several droplets would accumulate at the bottom of the sample volume on the surface of the floating piston if the cell was permitted to remain undisturbed. The overburden oil was then withdrawn until all the droplets evaporated into gas phase again. This procedure was repeated several times, yielding a more accurate dew point pressure. The results were presented in a pressure temperature diagram at the temperature of interest.

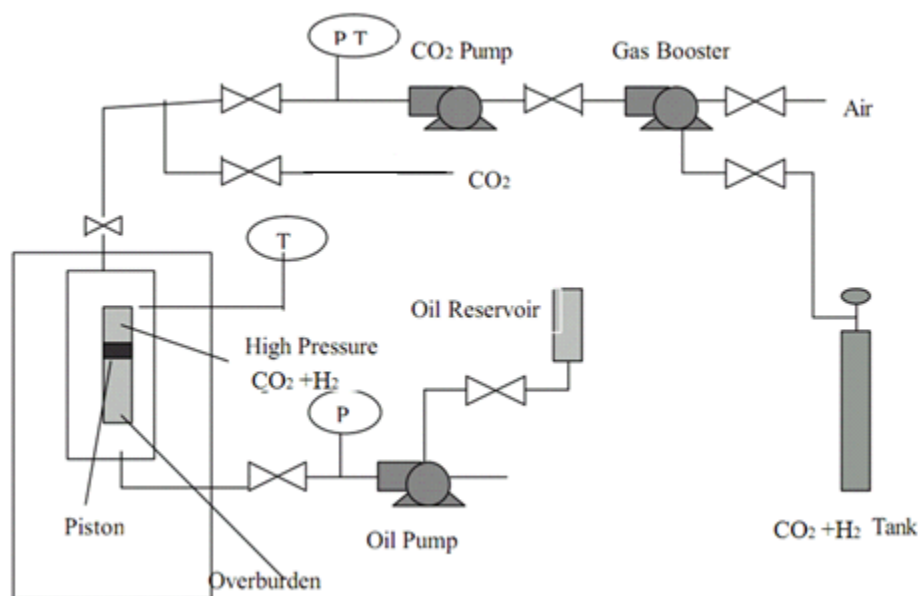


Figure 3. Diagram of high pressure, variable-volume, windowed cell (D. B. Robinson Cell)

2.3 PURIFICATION OF SAMPLES

TTBP (98%) was purchased from Sigma-Aldrich Company and was purified with ethanol before use. Recrystallization technique was used in the purification process. The impure TTBP (1 gram) was placed in an Erlenmeyer flask and a small volume of hot ethanol (absolute and anhydrous, 5ml) was added to the flask. The solution was kept in the Erlenmeyer flask warm in a hot oil bath (silicone oil) at the temperature of 373 K, and the solution was swirled to break up any lumps with a stirring rod. Occasionally there were impurities present in the solid that were insoluble, even at high temperature. The hot solution is filtered or decanted to remove the insoluble impurities. After the insoluble impurities were removed, the flask containing the hot filtrate was aside undisturbed to cool slowly to room temperature. After the flask had cooled to room temperature, it was placed in an ice bath to increase the yield of the solids. Once the

compound had completely precipitated from the solution, it was separated from the remaining solution by suction filtration using a Büchner funnel. The filter cake was removed from the funnel by carefully prying it from the filter using a spatula. The cake of crystals was still slightly wet with solvent and then it was dried thoroughly in a vacuum chamber overnight before measuring the weight of the solid material.

2.4 PURITY ANALYSIS OF SAMPLES

Differential scanning calorimetry (DSC) technique was used to qualitatively detect impurities. The difference in the amount of heat required to increase the temperature of the sample (purified TTBP) and reference (unpurified TTBP) were measured as a function of time. Both the sample and reference were maintained at nearly the same temperature throughout the experiment. When the sample underwent a physical transformation such as phase transition, e.g. as TTBP sample melted to a liquid, it would require more heat flowing to increase its temperature at the same rate as the reference. The melting process resulted in an endothermic peak in the DSC curve. Because the temperature range of a mixture of compounds melts was dependent on their relative amounts, less pure samples would exhibit a broadened melting peak that began at lower temperature than a pure compound would exhibit.

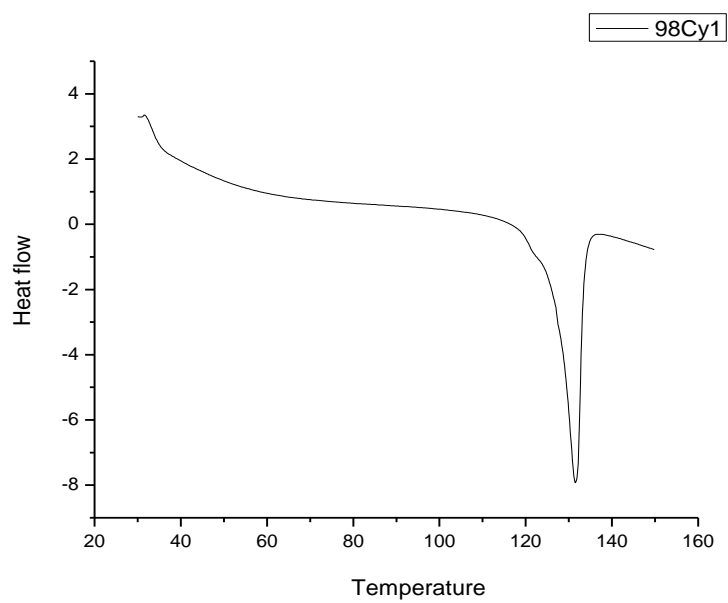


Figure 4. DSC of the unpurified TTBP

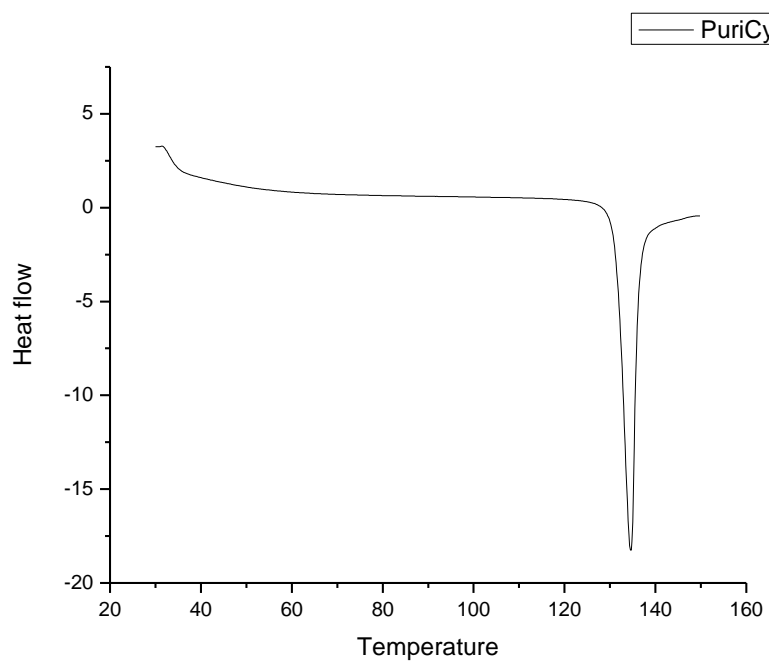


Figure 5. DSC of the purified TTBP

From the comparison we can find out that as the temperature approaches the melting point of TTBP (130 °C) both graphs exhibit a melting peak, in comparison, the second graph demonstrates a narrower peak, which indicates that the recrystallized TTBP is purer than the reference sample and could be used to run the phase behavior experiments.

2.5 CO₂ PHASE BEHAVIOR OF THE SOLID ABSORBENTS

The specific solids are identified from two classes, sugar acetates and tert-butylated aromatics that melt in the presence of high pressure CO₂ and absorb large amounts of CO₂ at room temperature. The phase behavior of these solids when mixed with a 50:50mol% gas mixture of CO₂ and H₂ was assessed because their use as a CO₂ selective compound was dependent on these solids melting in the presence of the mixture at a reasonable pressure (one that be attained in an IGCC plant), the molten solid preferentially absorbing CO₂ rather than H₂, and (most importantly) the CO₂ being released from the molten solid with a modest pressure drop that cause the solid to freeze in the form of the pure CO₂-philic compound. It is the ability to regenerate the CO₂-phile and recover the CO₂ at a pressure far above the near-atmospheric pressure regeneration pressures associated with conventional solvents that could enable a dramatic reduction in CO₂ compression costs required for CO₂ pipeline transport.

Glucose pentaacetate is the only candidate that melts in the presence of a CO₂-H₂ equimolar mixture at 25 °C when subjected to pressures as high as 10000 psi. However, the pressure required for the solid to melt is about 6000 psi, and melting occurred only in the 1-6wt% CO₂-phile range. This pressure is too high to be practical for an IGCC power plant

application because the H_2 and CO_2 mixture is generated at a pressure of only about 1000 psi. Compression of the gas mixture to 6000 psi to attempt this separation is not an option.

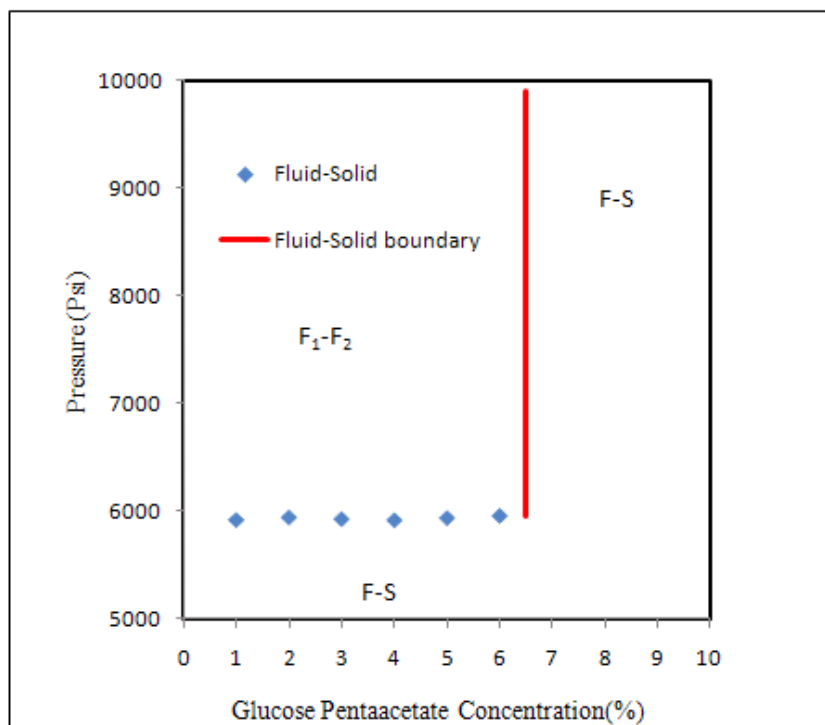


Figure 6. Pressure-composition diagram for glucose pentaacetate and H_2 - CO_2 system at 300.15 K

None of the solids melted in the presence of H_2 at pressures up to 10000 psi.

The following binary phase behavior results confirm that the candidates are indeed CO_2 -philic, melting at pressures of ~500-1000 psi.

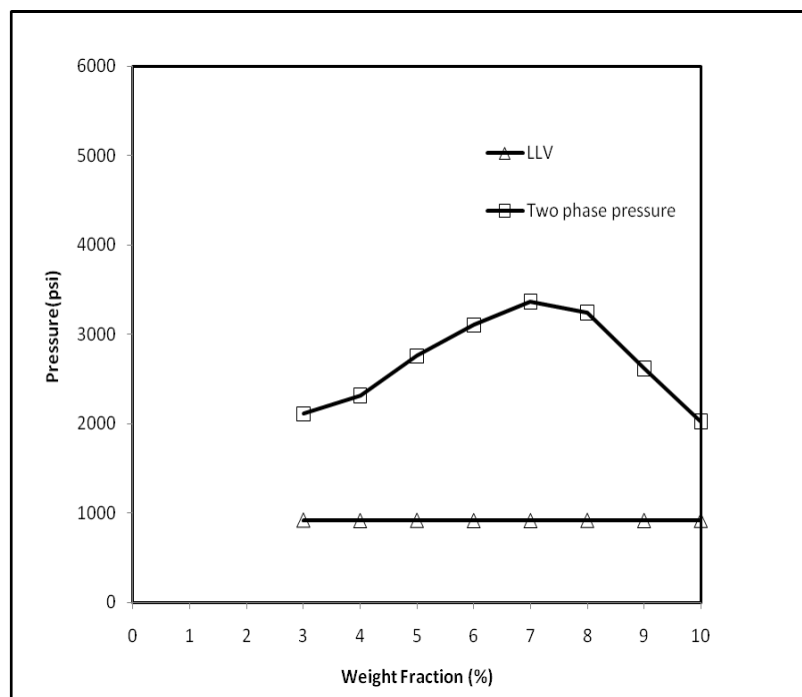


Figure 7. Pressure-composition diagram for β -D-ribofuranose 1,2,3,5-tetraacetate+CO₂ at 298 K

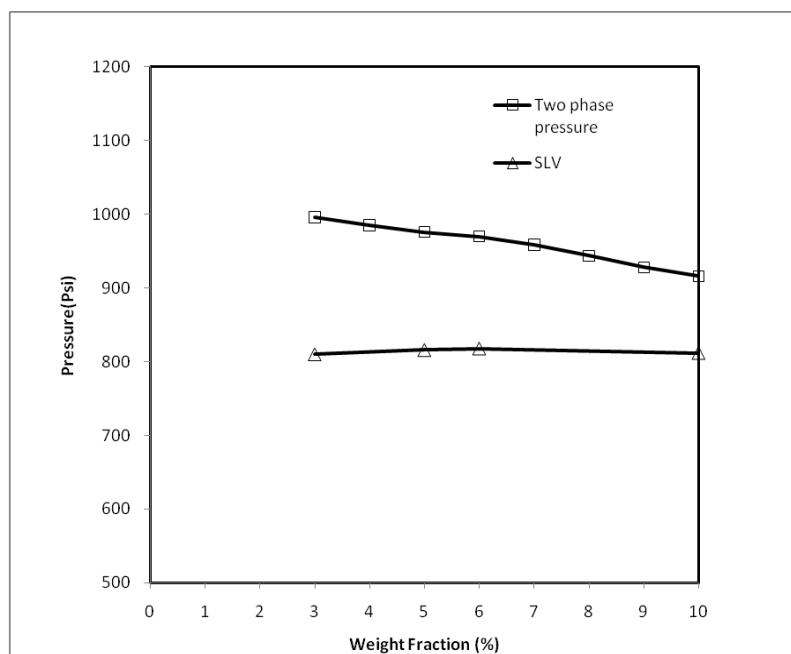


Figure 8. Pressure-composition diagram for sucrose +CO₂ at 298 K

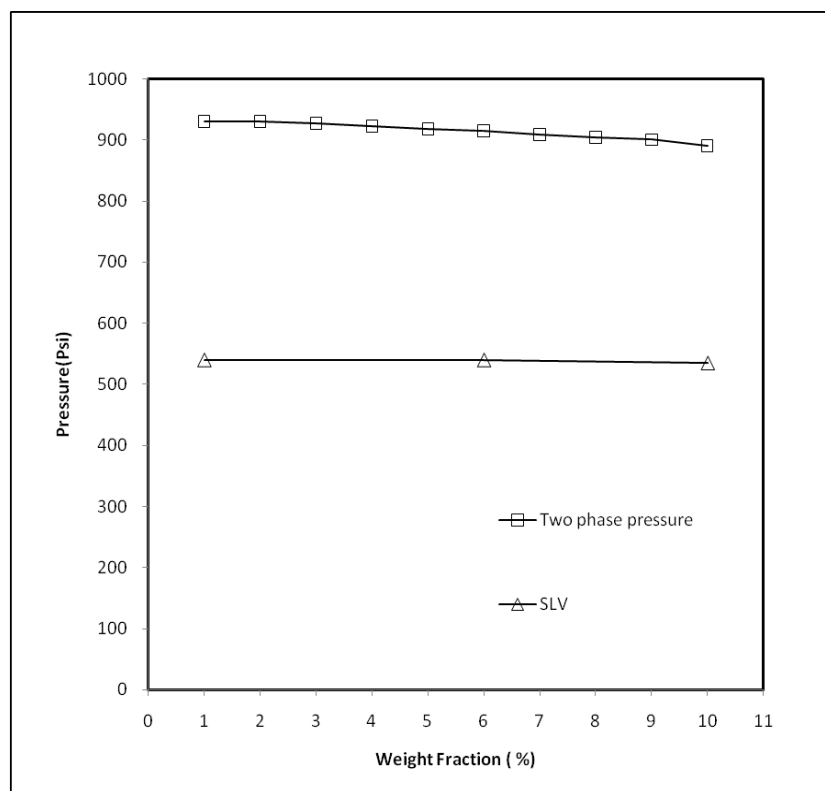


Figure 9. Pressure-composition diagram for 2-6-di-tert-butyl-4-methylphenol+CO₂ at 298.15 K

In summary, we did not find any CO₂-philic solids that could be applied as CO₂-selective capture absorbents at the IGCC power plant conditions for the CO₂-H₂ separation.

3.0 INTRODUCTION

CO₂ flooding of previously water-flooded oilfields has achieved a commercial success in the US. Approximately 200,000 barrels of oil are produced every day from CO₂ floods, which accounts for 4% of the US domestic oil production. CO₂ is effective at displacing oil from the portions of the reservoir through which it flows by a variety of mechanisms including pressure maintenance, oil swelling, oil viscosity reduction, and multiple-contact miscibility between CO₂ and crude oil if the CO₂ mixes with the oil at a pressure value greater than or equal to the minimum miscibility pressure (MMP) [8].

There are significant problems with this technology, however. After primary recovery and water-flooding, about 45% of the original oil in place, OOIP, is recovered. Although CO₂ is capable of displacing all of the oil from the portion of the sandstone through which it flows, only 15% of the original oil in place (which corresponds to ~27% of the 55% of the OOIP remaining after the water-flood), is recovered by CO₂. Further, 7500 scf of CO₂ is required to recover each barrel that is produced. At reservoir conditions, that corresponds to roughly 3.3 barrels of liquid or supercritical CO₂ per barrel of oil. The low viscosity of dense carbon dioxide is primarily responsible for this inefficiency. The unfavorable mobility ratio between the CO₂ and oil results in viscous fingering, which in turn leads to early CO₂ breakthrough and high CO₂ utilization ratios. The low viscosity of CO₂ also induces channeling, which is caused by permeability

inhomogeneities. The low density of CO₂ relative to oil and brine also exacerbates the low volumetric sweep efficiency due to gravity override of CO₂.

Although it is not possible to significantly alter the density of dense CO₂ via the addition of an additive or slight changes in injection pressure, it is possible to reduce the mobility of CO₂ flowing through porous media. The benefits of effective mobility reduction would be very significant. If the viscosity of CO₂ could be elevated to a value comparable to that of the oil being displaced, then the formation of viscous fingers would be suppressed even at high saturations of CO₂ in the porous media, yielding improved mobility control. If the viscosity of CO₂ could be increased, the relative proportion of CO₂ that would flow through high permeability channels would also be reduced. Based on data for recovery as a function of solvent/oil mobility ratio, it is reasonable to expect that the daily production rate of oil from CO₂ floods could increase substantially, and the fraction of the original oil in place that could be recoverable by CO₂ floods could increase from 15% to 40%.

3.1 REDUCING MOBILITY OF CO₂ IN POROUS MEDIA

The strategies that have been studied for this purpose include water-alternating-gas (WAG) relative permeability reduction, surfactant-alternating-gas (SAG) in-situ foam generation, and direct viscosity enhancement of CO₂. WAG is the industry standard for mobility control, SAG has been tested in the lab and at the pilot-scale, and direct thickeners are being investigated only at the lab scale.

3.1.1 DIRECT THICKENERS

The most challenging technique for decreasing the mobility of CO₂ is the addition of a dilute concentration of a “direct thickener” that can increase the CO₂ viscosity to a level comparable to that of the oil and brine. Thickening agents contain polar or ionic moieties that promote intermolecular interactions that lead to the formation of viscosity enhancing macromolecular structures in solution [9]. Unfortunately, these associating groups are CO₂-phobic. The strategy is to incorporate mildly CO₂-phobic associating groups into strongly CO₂-philic polymers. To date, only one direct CO₂ thickener capable of increasing the viscosity of CO₂ by a factor of ~2-10 at dilute concentrations of 1 wt% or less at MMP without the use of organic co-solvents has been identified. Former members in Dr. Enick’s research group designed a random copolymer of fluoroacrylate and styrene (polyFAST) that is effective at concentrations as low as 0.1 wt% [10]. The fluoroacrylate is extremely CO₂-philic and the styrene is a mildly CO₂-phobic group that causes intermolecular associations due to π - π stacking of the aromatic groups.

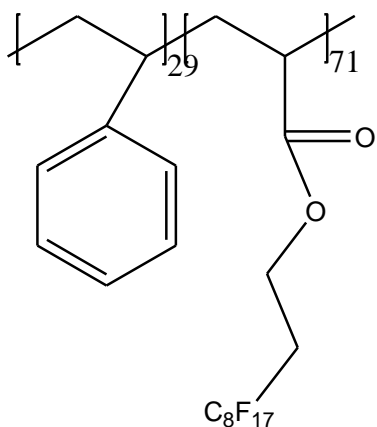


Figure 10. Structure of PolyFAST

3.1.2 WAG RELATIVE PERMEABILITY REDUCTION

Water-Alternating-Gas (WAG) remains the state-of-the-art technique for reducing the mobility of CO₂ as it flows through porous media. Typical cycle times range from months to a year and the volumetric ratio of water to dense CO₂ is roughly 1:1 to 2:1. Although applicable for most fields, WAG is not suitable for tight reservoirs or water-sensitive reservoirs; only continuous CO₂ injection is appropriate in these cases. The injection of large volumes of brine obviously does not make the CO₂ more viscous; rather it increases the water saturation and thereby decreases the dense CO₂ saturation within the pores. This, in turn, leads to a reduction in the relative permeability of CO₂, which tends to inhibit the formation of viscous fingers. Although WAG usually yields better results than continuously injecting CO₂, WAG floods still leave behind more than half of the oil left behind by waterflooding. Further, the WAG process requires the installation of water injection, production, collection and separation facilities, delays the injection of a specified volume of CO₂, and may inhibit the intimate contact of CO₂ and oil within the pores of the sandstone formation [11].

3.1.3 SAG RELATIVE PERMEABILITY REDUCTION

Rather than injecting alternating slugs of brine and CO₂, several researchers have proposed the alternate injection of surfactant solution and CO₂. The objective is to generate a foam (also referred to as an emulsion) as the CO₂ that is injected into the porous media mixes with the brine within the pores. The objective is to form a foam or emulsion within the pores in which the dense supercritical or liquid CO₂ is the high volume fraction, discontinuous phase, and the continuous brine phase wets the porous media and also forms surfactant-stabilized brine

lamellae that bridge the pore throats of the sandstone or limestone [12][13]. These CO₂ foams can exhibit a greatly reduced mobility in porous media relative to direct CO₂ injection or the WAG process. It was desired to form the foam in-situ by alternately injecting aqueous surfactant solution and supercritical CO₂ because the pressure drops associated with injecting a foam into the porous media would be too great. Unfortunately, field tests have yielded mixed results associated with surfactant adsorption losses on the rock porous medium [14]. Further, the CO₂ did not always flow into the same portion of the porous media where the previously injected surfactant solution flowed, therefore the foams were not always generated in the desired portions of the formation. In some cases, excellent foams were formed in-situ, but the foam mobility was too low, diminishing injection rates and dissuading field operators from further implementation.

3.2 SURFACTANTS DESIGN GUIDELINES

a). Efficacious at MMP Much progress has been made in the design of surfactants that dissolve in CO₂ at very high pressures, e.g. 20-150 MPa (3,000-20,000 psi) at ambient temperature. The surfactants used in this oilfield application, however, must be soluble in CO₂ at typical surface conditions where the surfactant would be added to the CO₂, and within the reservoir at reservoir temperature and typical MMP values. For example, at 25 °C, MMP values as estimated by numerous correlations are in the 1000-1500 psi range [15].

b). Non-ionics There are many CO₂-soluble ionic surfactants, but they require high pressures for dissolution (e.g. 7000 psi for ionic surfactants with twin oligovinyl acetate tails) in dilute concentrations of CO₂, which is well above the MMP.

c). Non-fluorous Although fluoroether and fluoroacrylate-based surfactants can exhibit high solubility in CO₂, they are usually very expensive.

d). CO₂-philic tails The surfactants must be identified with hydrocarbon-based tails that have been shown to be “CO₂-philic”, these tail attributes include highly branched (e.g. methylated, t-butylated), and/or highly oxygenated (e.g. PPG, PBG, acetates) tails with small number of carbons (e.g. <16)

e). Non-ionic hydrophiles PEG (polyethylene glycols) are common and effective non-ionic hydrophiles; PPG (polypropylene glycols) are slightly more CO₂-philic and less hydrophilic. Only PEG-based tails were used in this study.

f). More water-soluble than CO₂-soluble This allows the surfactant to enter the reservoir in the CO₂ phase and then partition strongly into the brine phase, where it can stabilize the CO₂-in-brine emulsion/foam in the pores of the sandstone or limestone.

g). Not too water-soluble Increasing the length of the hydrophile too much may stabilize the emulsion even more, but it makes the surfactant more difficult to dissolve in CO₂.

h). Low viscosity liquid surfactant Liquid surfactant are easier to introduce to a high pressure CO₂ line than high melting point solids. Further, they are likely to dissolve more rapidly.

4.0 PRELIMINARY WORK AND RESULTS

4.1 EXPERIMENT APPARATUS

The main objective of the foam stability apparatus is to determine whether a potential foaming surfactant with excellent solubility behavior in CO₂ is capable of forming stable foams with brine and CO₂ under realistic reservoir conditions. This is a further, more realistic investigation to evaluate a surfactant candidate's feasibility in real industrial application. Most of our tests require a dilute concentration of a surfactant, for example ~ 0.01~0.1 wt% [\[16\]\[17\]](#).

Surfactant solubility was determined from dew point data in the same manner as the CO₂-philic solid solubility was determined. The foam stability tests were conducted by first placing the liquid surfactant sample on top of the moving piston, inside the Pyrex phase behavior cylinder. The brine (5 wt% NaCl unless otherwise specified) was then poured into the glass cylinder. Then the Robinson cell is tightly sealed. Liquid CO₂, in an amount that provides the same volume as the brine, is introduced at ~1600 psi and room temperature. (Surfactant amounts are specified in wt% of the CO₂ phase.) The CO₂-brine interface position, initially at the middle of the cell with CO₂ above and brine below, is recorded. Then the system is then agitated in the vertical position with a flexible, metal, multiple slotted-fin impeller turning at 2500 rpm for 20 minutes. This provides intense mixing and creates an opaque white emulsion that fills the entire

cell. Once the mixing is stopped, data collection begins. The foam would collapse toward the interface from the top as a clear zone of CO₂ appears above the emulsion as bubbles coalesce, and the bottom as the liquid films of brine drain into an excess phase. Therefore the stability of the emulsion can be represented by two curves, one tracing the collapse of the emulsion at the CO₂-emulsion interface, and one following the collapse of the emulsion at the brine-emulsion interface. The following graph shows the whole process of a foam stability test for an excellent surfactant which lasts for 5 hours and does not yield a clear CO₂ zone in this period of time. (SAG studies have demonstrated that surfactants that perform well in this type of stability test typically perform well in generating foams in porous media.

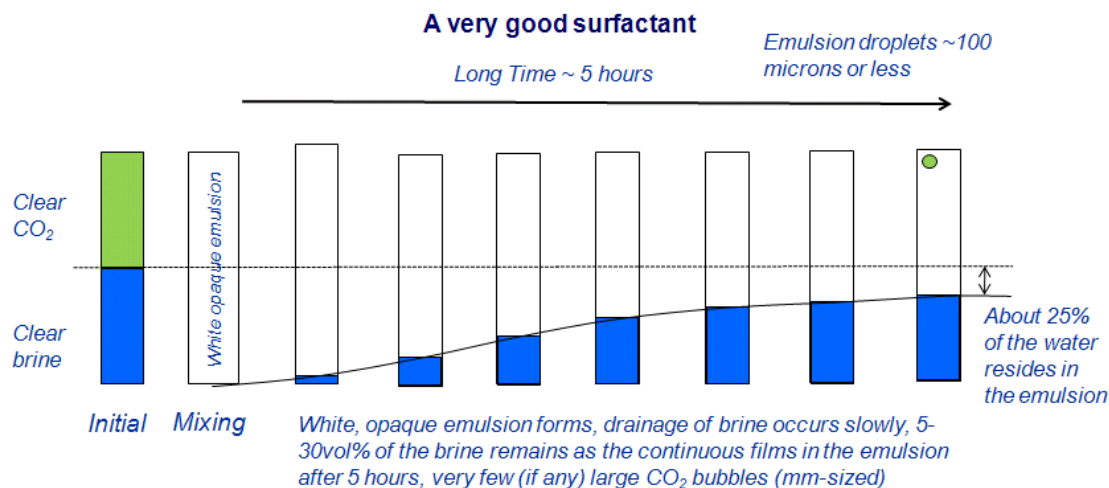


Figure 11. Foam stability test cartoon description

4.2 SOLUBILITY AND FOAM STABILITY TESTS

The objective of these tests were to identify commercially available, inexpensive, non-ionic surfactants that are capable of dissolving in CO₂ in dilute concentration at typical MMP

conditions and, upon mixing with brine in a high pressure windowed cell, stabilizing CO₂-in-water or CO₂-in-brine emulsions (a.k.a. foams in petroleum engineering literature). Most of the surfactants that were tested are hydrocarbon-based non-ionics that are commercially available in large quantities at prices in the \$0.75-\$3/l b range. The candidates selected for the study include:

1. Branched alkylphenol ethoxylates

- (a). Dow octylphenol Triton X 100
- (b). BASF octylphenol Lutensol OP 10
- (c). Huntsman octylphenol Surfonic OP 100 and 120
- (d). Dow nonylphenol Tergitol NP 4, 6, 9, 12, and 15
- (e). Huntsman nonylphenol Surfonic N 85, 100, 120, 150, and 200
- (f). Huntman dodecylphenol DDP 100 and 120

2. Linear alkylphenol ethoxylates – Stepan nonylphenol Cedepal CO 630 and 710

3. Branched alkyl ethoxylates

- (a). Dow dodecyl (i.e. trimethyl nonyl) Tergitol TMN 6 (10% water)
- (b). BASF decyl Lutensol XP 70 and 80
- (c). BASF Lutensol branched C₁₃ oxoalcohol with 8 or 10 EO groups TO 8 and 10
- (d). Huntsman isotridecyl ethoxylate TDA 8 and 9
- (e). Huntsman nonylphenol Surfonic N 85, 100, 120, 150, and 200
- (f). Empilan KR 6 and 8, the 6- and 8-mole ethoxylate of a slightly branched (α -methyl) primary C₉₋₁₁ alcohol

4. Monolaurate polyethyleneglycol – Sigma Aldrich PEG monolaurate 600

5. Linear alkyl ethoxylates/Brij surfactants

- (b). Sigma Aldrich decaethyleneglycol monododecylether, Brij surfactant C₁₂E₁₀

4.2.1 BRANCHED ALKYLPHENOL ETHOXYLATES

- and 120 branched octylphenol ethoxylates:

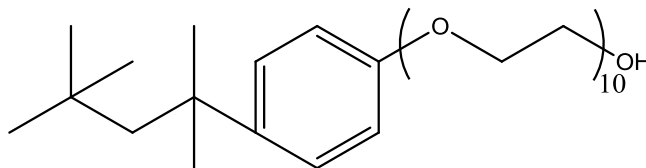


Figure 12. DOW Triton X 100, BASF Lutensol OP 10 and Huntsman octylphenol Surfonic 100 and 120

Solubility result:

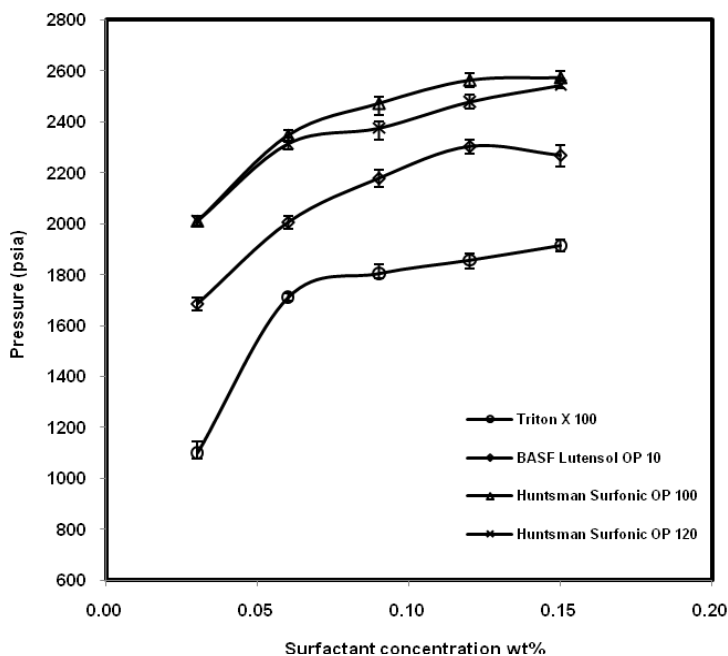


Figure 13. Solubility of Dow Triton X 100, BASF Lutensol OP 10 and Huntsman octylphenol Surfonic OP 100 and 120 in CO₂ at 25 °C

Dow Triton X-100, BASF OP 10, and Huntsman OP 100 were expected to have a similar solubility because their structure is reported to be identical. But based on the figure above, the solubility decreases in the following order: Dow, BASF, Huntsman. This may be attributable to different polydisperse mixtures of the PEG hydrophile (“10” nominally represents the average number of EO units in the tails, which are actually polydisperse blends of PEG), different water contents (all report no water), or the presence of impurities that could act as co-solvents or anti-solvents. The surfactants were used as is from the manufacturer, however; resources were not available to characterize all of the surfactants. As the case with all of the surfactants investigated in this study, the cloud point pressure increases with concentration. As for Huntsman OP 100 and 120, the Huntsman OP 120 is more soluble in CO₂.

Foam stability result:

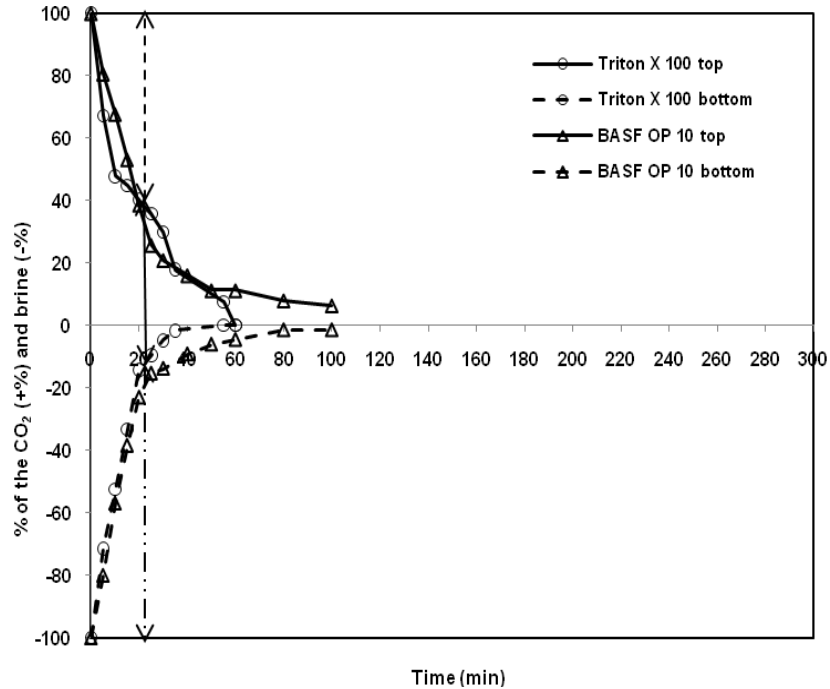


Figure 14. 0.04 wt% Triton X-100 and 0.03% BASF OP 10 in CO₂ at 1300 psi and 25 °C, with a brine (5 wt% NaCl)/CO₂ volume ratio 1:1.

The Triton X 100 and BASF OP 10 yielded very similar foam stability results. Consider Triton X 100 as an example. At 20 minutes, 85 vol% of the original brine is in a clear brine zone at the bottom of the cell (dash-dot solid arrow), 60 vol% of the CO₂ is in a clear CO₂ zone at the top of the cell (dash arrow), and 40% of the CO₂ and 15% of the original brine are in the middle-phase white, opaque, CO₂-in-brine emulsion in the center of the sample volume (solid arrow). But Huntsman OP 100 and 120 do not foam in this study when used at a concentration of 0.2%.

2). Dow Tergitol NP branched nonylphenol ethoxylates:

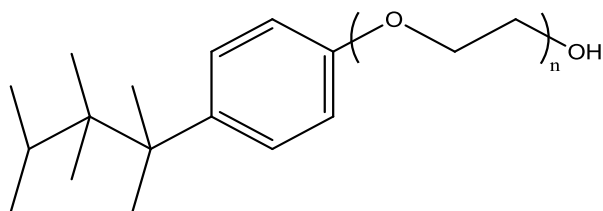


Figure 15. DOW Tergitol NP Series, $n = 4-15$

Solubility result:

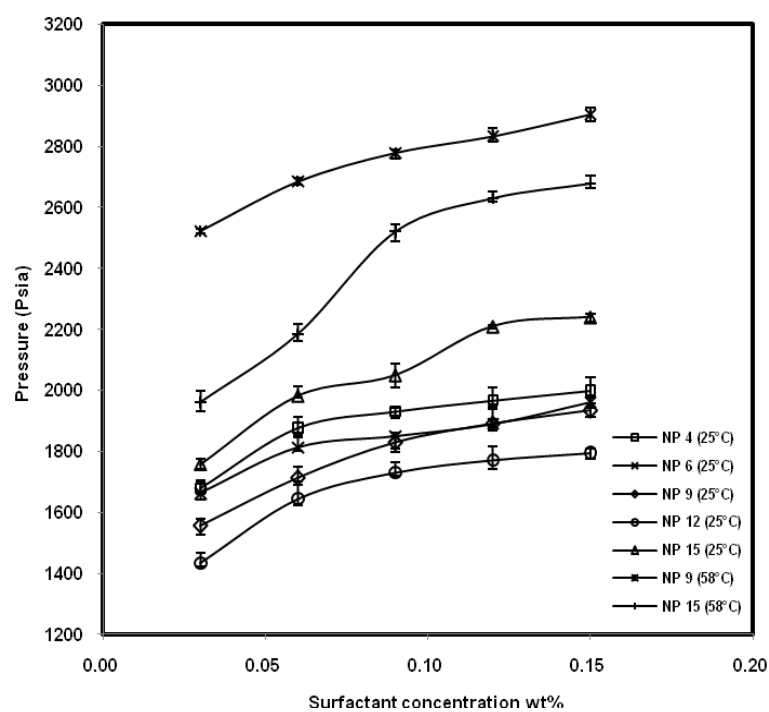


Figure 16. The effect of the average number of EO groups on the solubility of Tergitol NP series of branched, nonylphenol ethoxylates in CO_2 at 25 °C and 58 °C

NP 4 and 6 are not water soluble, but NP 9, 12, and 15 are water soluble. NP surfactants with 4, 6, 9, 12 and 15 EO repeat units were all found to be slightly soluble in CO₂. The branched nonylphenol group is hydrophobic and CO₂-philic, while the polyethylene glycol group is slightly CO₂-philic and strongly hydrophilic. The most CO₂-phobic portion of the surfactant structure is the terminal hydroxyl group (-OH). As the length of the poly(ethylene glycol) increases from 4 to 6 to 9, the surfactant becomes more CO₂ soluble, as evidenced by a decrease in the cloud point pressure at a specified composition (i.e. the cloud point locus shifts to lower pressure values). Apparently, as the poly(ethylene glycol) increases in length from 4 to 9 EO units, the molecule becomes more CO₂-philic because the CO₂-philic alkyl segment remains unchanged, the slightly CO₂-philic PEG segment increases, and the CO₂ phobic hydroxyl group remains unchanged. The results for the NP surfactants with 9 and 12 EO groups are comparable, with both surfactants slightly more CO₂-soluble than the NP 6. At 25 °C and 1300 psi for example, both NP 9 and NP 12 are about 0.04 wt% soluble in CO₂. As the PEG increases from 9 to 12 EO groups, the increasing molecular weight of the surfactant has begun to diminish the CO₂ solubility of the surfactant. The cloud point pressure values then increase as the length of the PEG segment increases to 15 EO groups as the increased molecular weight of the surfactant continues to lessen its solubility in CO₂. NP surfactants with even greater numbers of EO groups would be expected to be even less CO₂ soluble than NP 15.

Foam stability result:

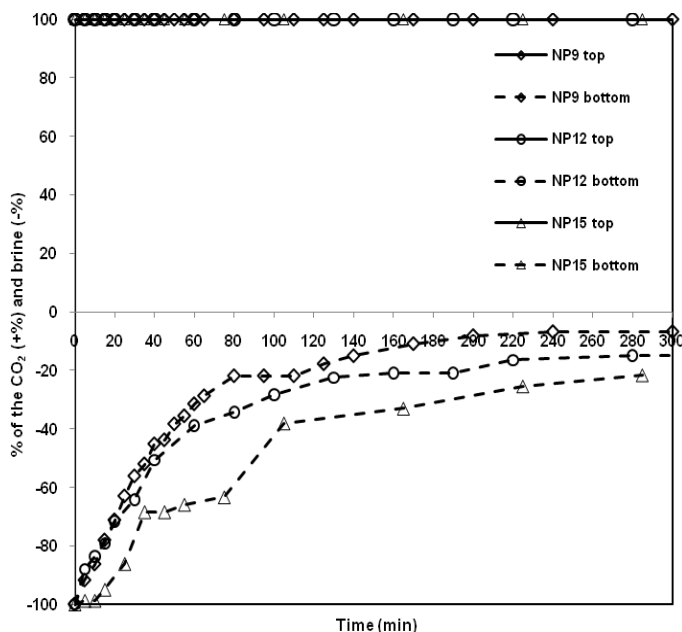


Figure 17. Foam stability associated with the Dow Tergitol NP series foams at 1300 psi and 25 °C, with a brine (5wt% NaCl)/CO₂ volume ratio 50:50

NP 4 and NP 6 are not water-soluble, and neither one was capable of stabilizing CO₂-in-brine emulsions at concentrations up to 0.02 wt%. Excellent results were obtained with the NP 9, 12, and 15 at concentrations of 0.04 wt%, 0.03 wt%, and 0.03 wt% of the CO₂, respectively. In each case, a clear brine zone began to emerge below the emulsion as soon as the mixing ceased, but no clear zone of CO₂ appeared above the emulsion after 300 minutes. At 300 minutes, approximately 10 vol%, 15 vol% and 20 vol% of the brine was retained within the emulsion along with all of the CO₂ for the NP 9, 12, and 15 surfactants. Therefore the emulsions for the NP 9, 12, and 15 surfactants contained CO₂: brine volume ratios of 100:10, 100:15, and 100:20 after 300 minutes.

3). Huntsman nonylphenol Surfonic series:

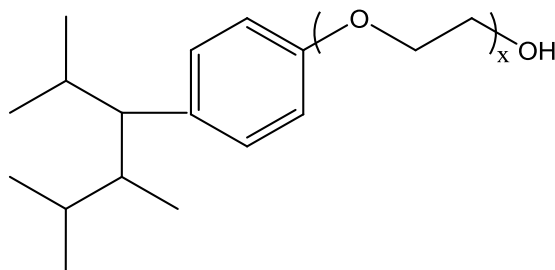


Figure 18. Huntsman Surfonic N 85, 100, 120, 150, 200, $x = 8.5, 10, 12, 15, 20$

Solubility result:

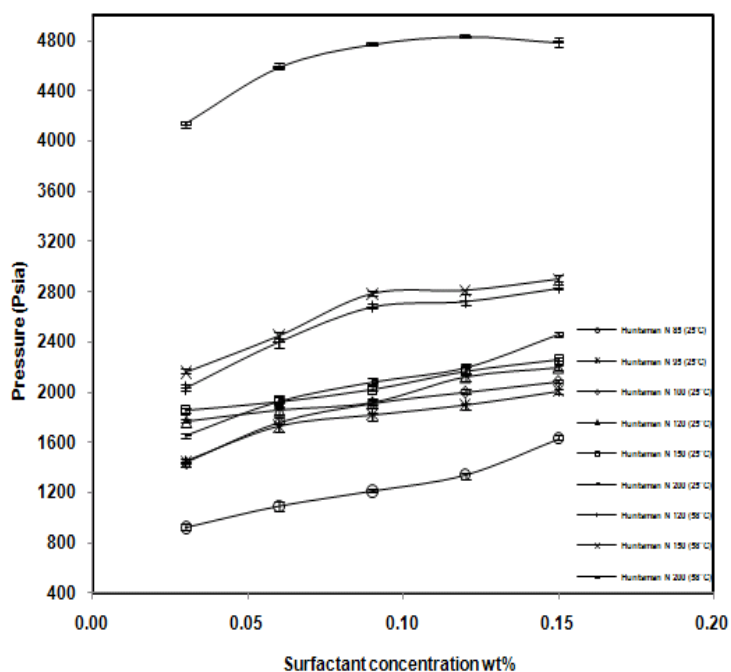


Figure 19. The effect of the average number of EO groups on the solubility of Huntsman N series of branched, nonylphenol ethoxylates in CO₂ at 25 °C and 58 °C

Huntsman N 85 exhibits a solubility of about 0.10 wt% in CO₂ at 25 °C and 1300 psi. Huntman Surfonic N 85 and Tergitol NP 9 are both branched nonylphenol ethoxylates with ~9 EO units, but the Huntsman surfactants were more CO₂-soluble. The reason for this difference is

not apparent. Surfonic N 95 and N 100 cloud point pressure values increased with the number of ethoxylate group, probably due to the entropic effect of high molecular weight. Both cloud point pressure loci are higher than MMP (1300 psi) at 25 °C, even at the concentration of 0.02 wt%. Further, foaming stability investigations for Surfonic N 95 and N 100 at dilute concentrations show that neither of them could form stable foams. Better foam stability was attained for Surfonic N 120 and N150, although the solubility at room temperature was less than the N 85, N95 and N 100 surfactants. Therefore Huntsman Surfonic N 120, 150, and 200 are viable foaming agents.

Foam stability result:

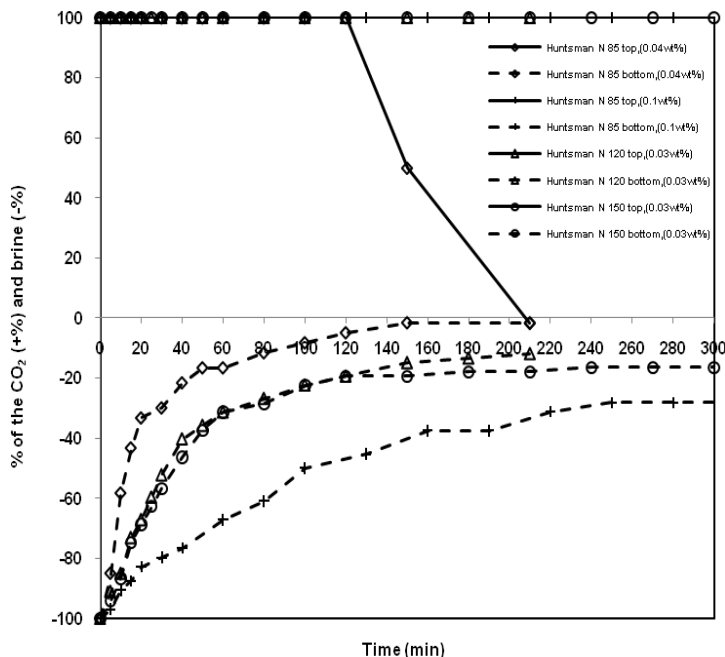
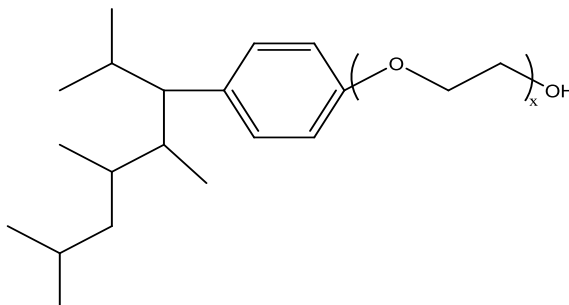


Figure 20. Huntsman Surfonic N series foams at 1300 psi and 25 °C, with a brine(5 wt% NaCl)/CO₂ volume ratio 50:50; 0.04 wt% N 85, 0.03% N 120 and N 150

4). Huntsman dodecylphenol DDP 100 and 120:



33

Solubility result:

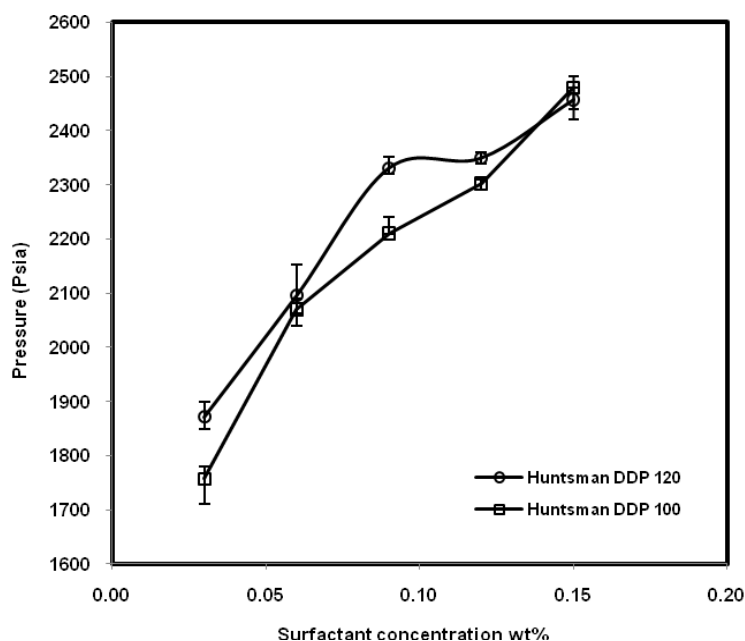


Figure 22. The solubility of Huntsman Surfonic DDP 100 and 120 branched, mixed isomeric, dodecylphenol ethoxylate in CO₂ at 25 °C

This surfactant is slightly less CO₂ soluble than Huntsman's branched, mixed isomeric, nonylphenol N 120. Both surfactants have identical hydrophiles with an average of 12 EO groups; therefore the diminished solubility is attributable to the three additional carbons in the branched alkyl chain of the DDP 120.

Foam stability result:

Huntsman DDP 120 was less soluble in CO₂ than the NP 120 surfactant and was therefore tested at 0.02 wt% in CO₂. At this concentration, the emulsion collapsed immediately when the mixing stopped.

4.2.2 LINEAR ALKYLPHENOL ETHOXYLATES-STEPAN NONYLPHENOL CEDEPAL CO 630 AND 710

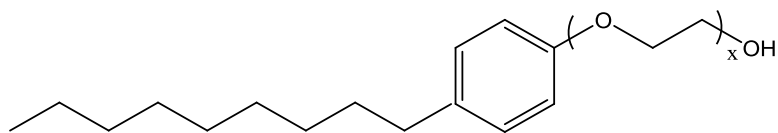


Figure 23. Stepan Cedepal CO 630 and 710, $x = 10, 10.5$

Solubility result:

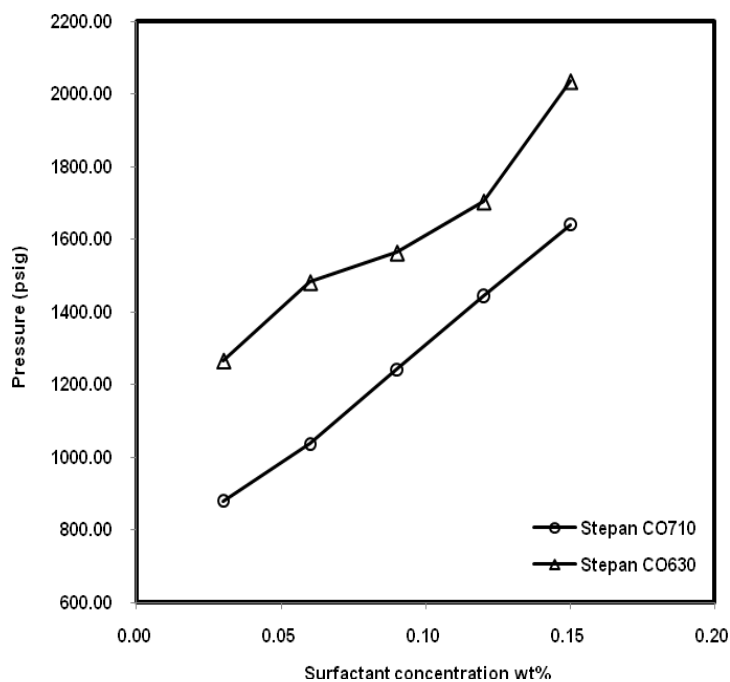


Figure 24. Solubility of Stepan CO 630 and 710 in CO₂ at 25 °C

The slight increase in the number of EO groups from 10 to 10.5 results in a very significant decrease in cloud point pressure. This difference is far beyond that expected for such

a modest change in structure. At a typical MMP of ~1300 psi at 25 °C, about 0.1 wt% Stepan CO710 dissolves in CO₂, while only about 0.03wt% Stepan CO 630 is dissolved. The results for CO 710 with 10.5 EO groups are comparable to the branched nonylphenol surfactants with a similar number of EO groups, Dow Tergitol NP 9 and Huntsman Surfonic N 100. At these very dilute concentrations of <0.2 wt%, the degree of branching in the hydrocarbon tails does not appear to dramatically alter the CO₂ solubility of the surfactant.

Foam stability result:

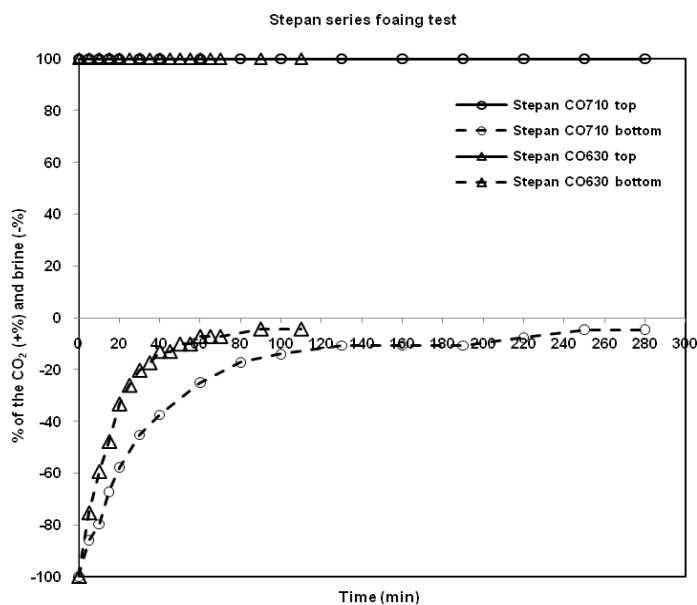


Figure 25. 0.03 wt% Stepan CO 710 and CO 630 in CO₂ at 1300 psi and 25 °C, with a brine (5wt%NaCl)/CO₂ volume ratio 50:50

The foam stability of Stepan CO 710 is greater than that of CO 630 at the same concentration 1300 psi and 25 °C. This Stepan CO 710 result was comparable to the stability associated with the branched alkylphenol ethoxylates Dow NP 9 at 0.04 wt% and Huntsman N 85 at 0.10 wt%.

4.2.3 BRANCHED ALKYL ETHOXYLATE

Given the environmental concerns associated with the decomposition of nonylphenol ethoxylates that has resulted in their ban in Europe and Canada, all major surfactant manufacturers are currently designing and offering branched ethoxylated alcohols (i.e. branched alkyl ethoxylates) especially since these companies anticipate a similar ban in less than five years in the US.

- 1). Dow dodecyl (i.e. trimethyl nonyl) Tergitol TMN 6 (10% water)

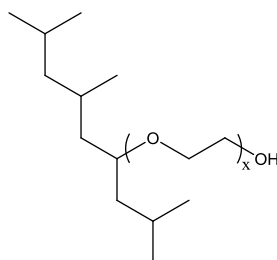


Figure 26. DOW Tergitol TMN Series, $x = 6$

Solubility result:

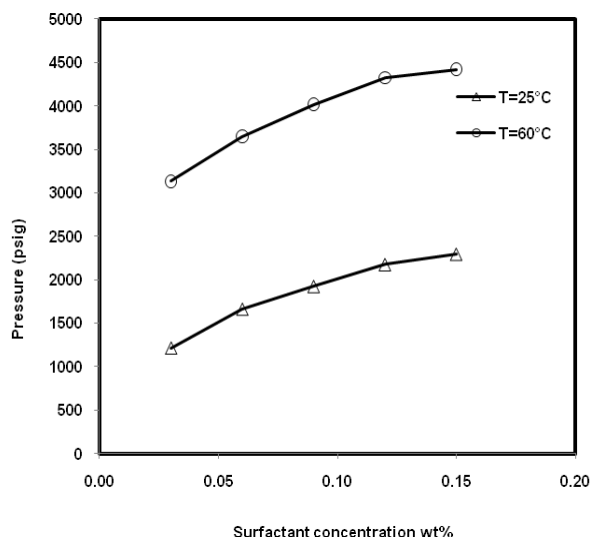


Figure 27. DOW Tergitol TMN-6 branched trimethylnonyl ethoxylate (10% water) in CO₂ at 25 °C and 60 °C.

The solubility of Dow's branched C₁₂ TMN 6 alkyl ethoxylate is tested at two different temperatures and the result indicates that the solubility of these nonionic surfactants in CO₂ decreases with temperature as expected. The reason that high temperature solubility result is necessary is that the temperature of certain reservoirs operated by a company interested in this technology is about 60 °C. Under current surfactant screening stage, most tests are still run at ambient temperature.

Foam stability result:

The TNM 6 foaming emulsion collapsed with several seconds.

2). BASF Lutensol XP 70 and 80, x=7 and 8

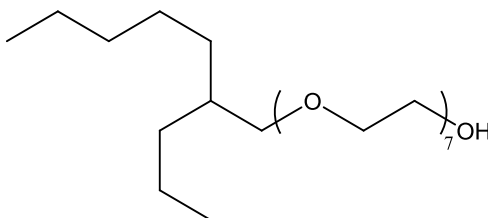


Figure 28. BASF Lutensol XP 70 and 80, x=7 and 8 (C10 alkyl chain structure is proprietary)

Solubility result:

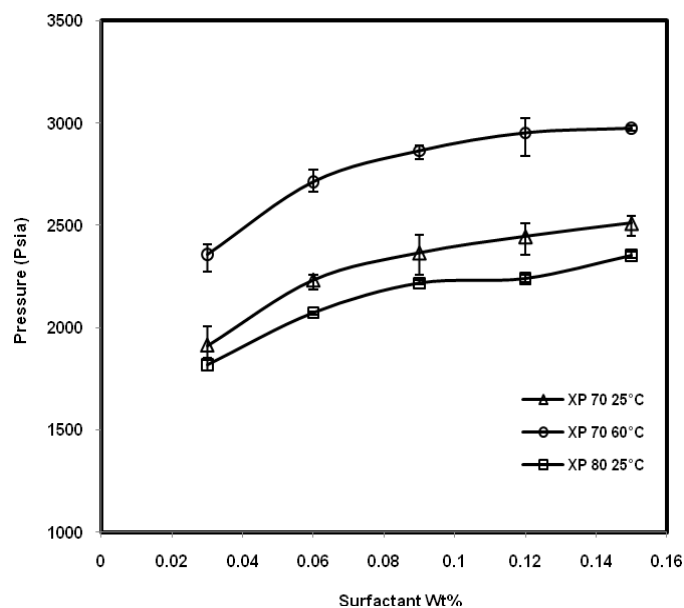


Figure 29. The solubility of BASF XP 70 and XP 80 in CO₂ at 25 °C and 60 °C

The solubility of BASF's C10 XP 70, 80 alkyl ethoxylates are tested at 25 °C and 60 °C. As temperature increases, the solubility of XP 70 in CO₂ decreases as expected. Because XP 80 has more EO groups, it is more soluble in CO₂ than XP 70.

Foam stability result:

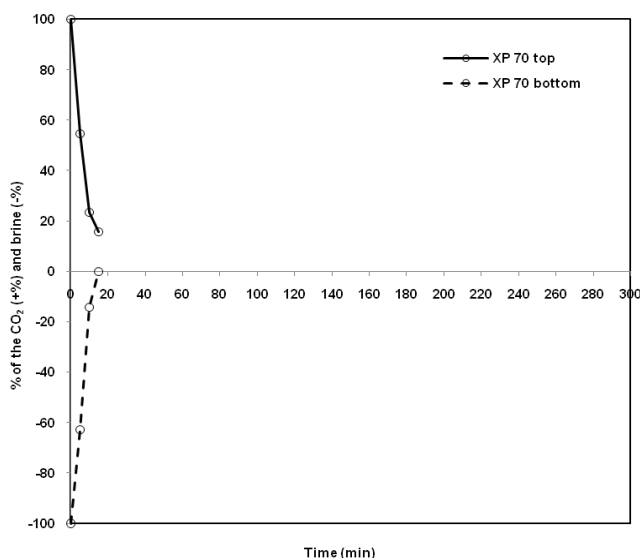


Figure 30. Foam stability of 0.04 wt% BASF XP 70 in CO₂ at 1300 psi and 25 °C, with a brine (5 wt% NaCl)/CO₂ volume ratio 1:1

The BASF XP-70 foam emulsion just lasted about 15min and collapsed and TMN 6 collapsed within few seconds. The reason for this poor performance may be that these surfactants that did not contain a phenol group (i.e. aryl group, benzene ring) between the alkyl group and the ethoxylated segment, such as BASF Lutensol XP 70 and Dow Tergitol TMN 6, yielded emulsions that were substantially less stable than those generated with alkylphenol ethoxylates. It may be that the $\pi - \pi$ stacking of the benzene rings of adjacent surfactant molecules at the CO₂-brine interface enables the surfactants to stack more efficiently and stabilize the aqueous films. This has not been confirmed, however.

3). BASF Lutensol branched C₁₃ oxoalcohol and Huntsman isotridecyl ethoxylate

Huntsman presents the structure of their TDA surfactants as shown in [Figure 31](#), but while it is known that BASF TO surfactants are proprietary branched C₁₃ oxoalcohol ethoxylates with 8 or 10 EO groups; the specific structure is not available

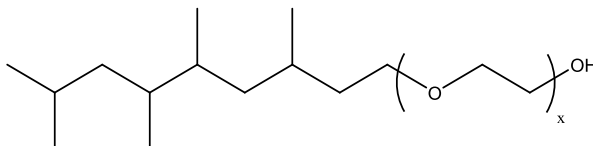


Figure 31. Huntsman isotridecyl ethoxylate TDA 8 and 9, x = 8 and 9, Huntsman are branched C₁₃ alcohol ethoxylates

Solubility result:

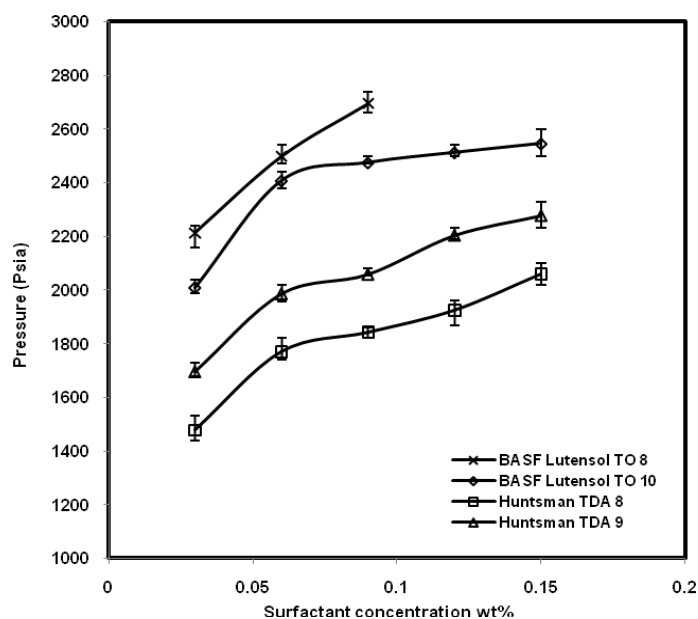


Figure 32. BASF Lutensol TO 8 and 10 and Huntsman TDA 8 and 9 in CO₂ at 25 °C

Foam stability result:

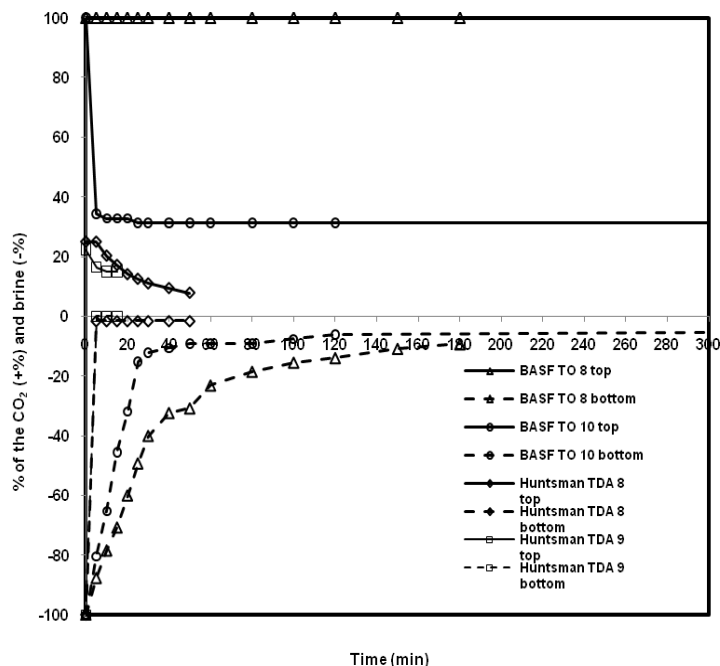


Figure 33. Foam stability of 0.03 wt% BASF TO 8, 10, and Huntsman TDA 8, 9 in CO₂ at 1300 psi and 25 °C, with a brine(5wt%NaCl)/CO₂ volume ratio 1:1

4). Huntsman Empilan KR 6 and 8, the 6- and 8-mole ethoxylate of a slightly branched (α -methyl) primary C₉₋₁₁ alcohol

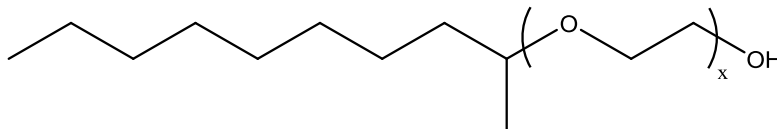


Figure 34: Huntsman Empilan KR 6 and 8, the 6- and 8-mole ethoxylate of an α -methyl primary C₉₋₁₁ alcohol

Solubility result:

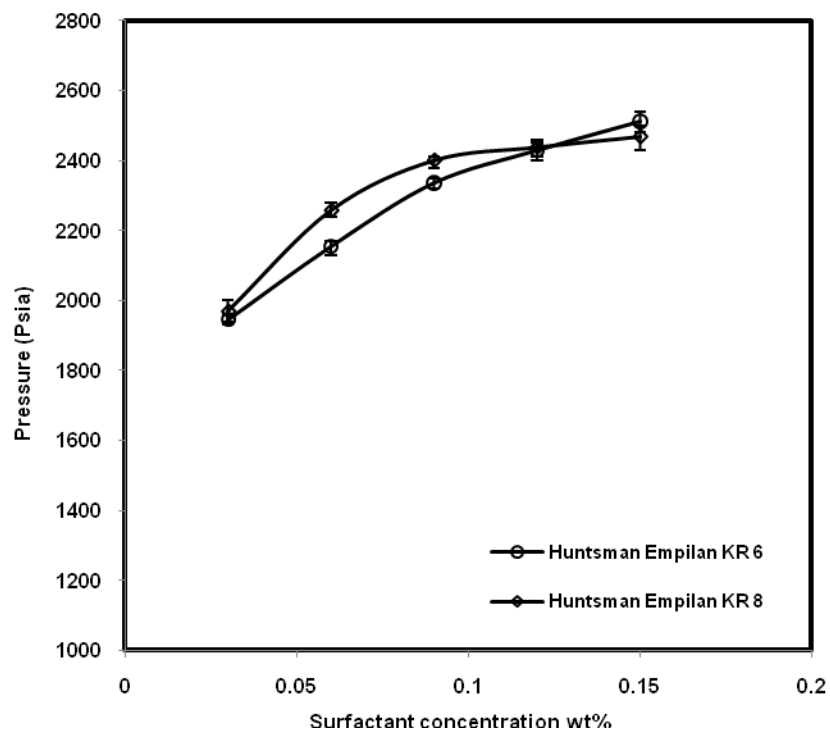


Figure 35. Huntsman Empilan KR 6 and 8

Foam stability result:

Huntsman Emplian KR 6 and does not foam

4.2.4 MONOLAURATE POLYETHYLENEGLYCOL

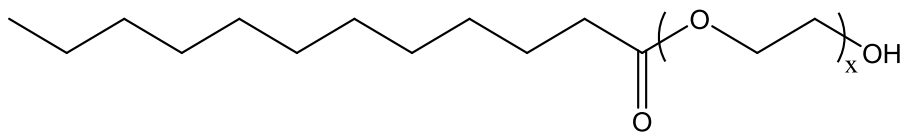


Figure 36. Sigma Aldrich PEG monolaurate 600, $x = 9$

Solubility result

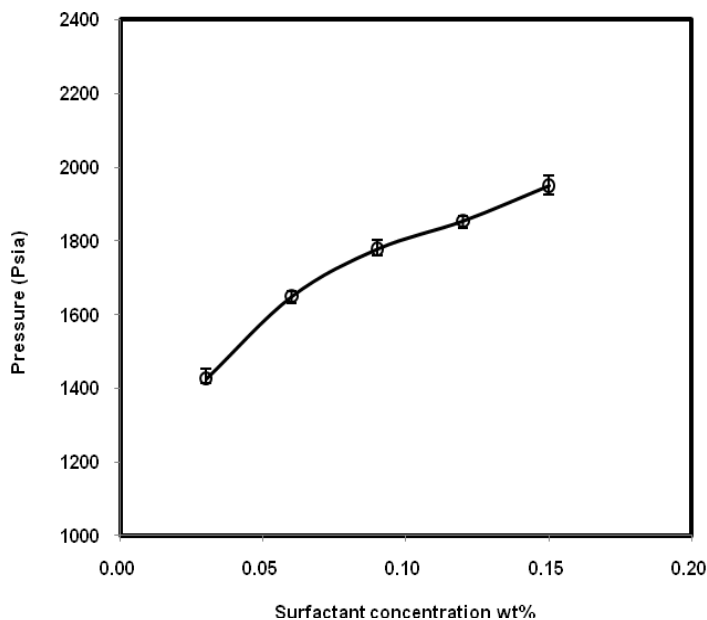


Figure 37: Solubility of monolaurate PEG in CO₂ at 25 °C

Foam stability result:

Monolaurate polyethyleneglycol at the 0.03 wt% in CO₂ at 1300 psi and 25 °C does not foam.

4.2.5 LINEAR ALKYL ETHOXYLATES/BRIJ SURFACTANTS

1. Linear alkyl ethoxylates/Brij surfactants

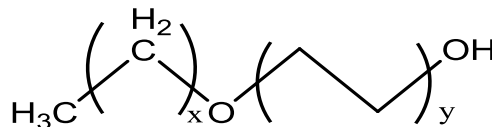


Figure 38. Huntsman L 12-6 and 12-8, the six-mole and eight-mole ethoxylates of linear, primary C₁₀₋₁₂ alcohol, Brij surfactants C₁₁E₆ and C₁₁E₈. Sigma Aldrich decaethyleneglycol monododecylether, Brij surfactant C₁₂E₁₀

Solubility result

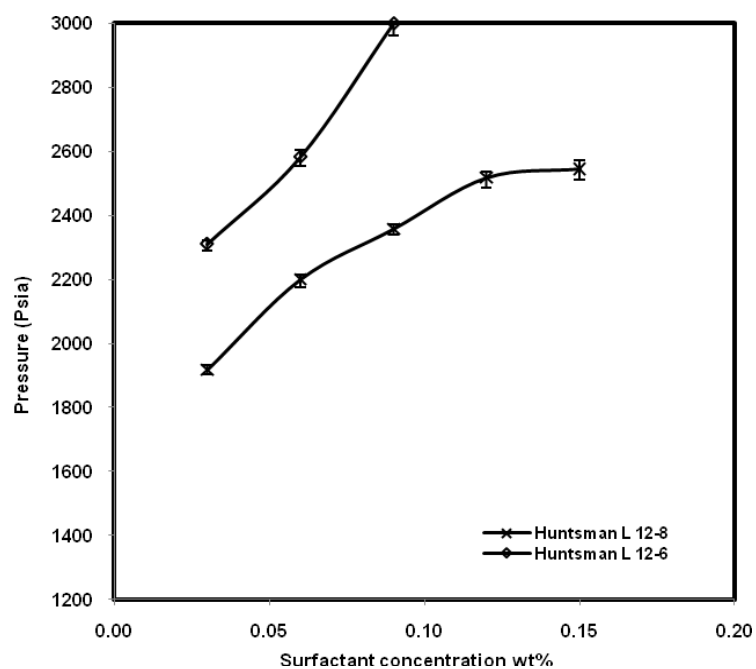


Figure 39: Huntsman L12-8 and L12-6 in CO₂ at 25 °C

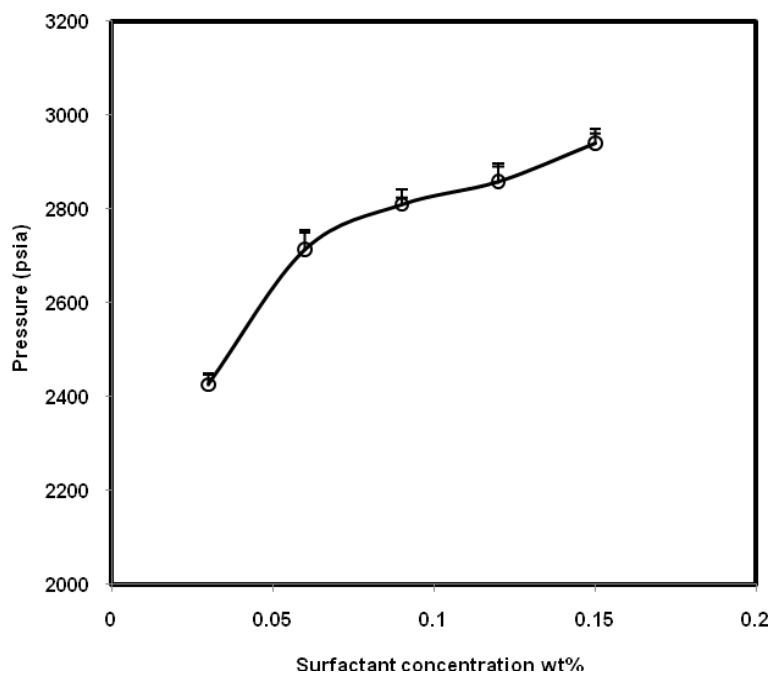


Figure 40: SigmaAldrich decaethyleneglycol monododecylether

Foam stability result:

None of the linear “Brij” type surfactants were capable of stabilizing CO₂-in-brine emulsions.

In general, the most promising surfactants for stabilizing CO₂-in-brine emulsions are very water-soluble, slightly CO₂-soluble, branched alkylphenol ethoxylates, such as the Huntsman Surfonic N 85, 100, 120, and 150, and the Dow Tergitol NP 9, 12 and 15. The best results are obtained using surfactants with the longest EO groups that still retain CO₂ solubility at test conditions. It is not yet evident, however, why subtle changes in tail structure can affect the performance of the surfactant. For example, the branched octylphenol ethoxylate Dow Triton X 100 produces a much less stable emulsion than the branched, mixed isomeric, nonylphenol ethoxylate Dow Tergitol NP 9, while the performance of the linear nonylphenol ethoxylate Stepan Cedepal 710 was comparable to the Dow Tergitol NP 9 surfactant. Further, the surfactants that do not contain a phenol group (i.e. aryl group, benzene ring) between the alkyl group and the ethoxylated segment, such as BASF Lutensol XP 70 and Dow Tergitol TMN 6, yielded emulsions that were substantially less stable than those generated with alkylphenol ethoxylates. (Nonetheless these surfactants may yield acceptable low mobility foams in porous media, therefore it is critical to keep these surfactants in on-going and future studies, especially because they are more environmentally benign than nonylphenol ethoxylates.) It may be that the $\pi - \pi$ stacking of the benzene rings of adjacent surfactant molecules at the CO₂-brine interface enables the surfactants to stack more efficiently and stabilize the aqueous films.

4.3 SACROC BRINE FOAM TESTING

The ability of branched, mixed isomeric, nonylphenol ethoxylates to stabilize CO₂-in-brine emulsions was tested using SACROC brine at typical CO₂ flooding conditions of 58 °C and 3200 psi. A produced brine sample (specific gravity 1.059, pH 6.84) from this West Texas field operated by KinderMorgan containing 83078 ppm TDS (major constituents 48762 Cl⁻, 25850 Na⁺, 916 Mg⁺², 4345 Ca⁺², 274 Sr⁺², 2133 HCO³⁻, 798 SO₄⁻²) was filtered with 0.22 micron cellulose acetate paper prior to use. Cloud points tests using 1wt% surfactant mixed with the brine indicated that Huntsman Surfonic 100 and Dow Tergitol NP 12, 15 were soluble in the SACROC brine at 58 °C, while branched nonylphenol ethoxylates with fewer EO groups in the tails were not soluble in the brine. The foam results for the SACROC brines obtained with the Huntsman and Dow surfactants are provided in Figures 42. The surfactants with the longer EO tails, Huntsman Surfonic N 150 and Dow Tergitol NP 15, yielded foams that were more stable than the analogous surfactants with 12 EO groups. The foams were less stable than those obtained using the same surfactants in the screening tests due to the increased temperature (58°C vs 25°C), the increase in the TDS of the brine (83078 ppm vs 50000 ppm), and the mixed ions present in the SACROC brine (Cl⁻, Na⁺, Mg⁺², Ca⁺², Sr⁺², HCO³⁻ , SO₄⁻² vs Na⁺, Cl⁻) [18]. Nonetheless the foam stability results indicate that these surfactants do have the potential to form foams at reservoir conditions.

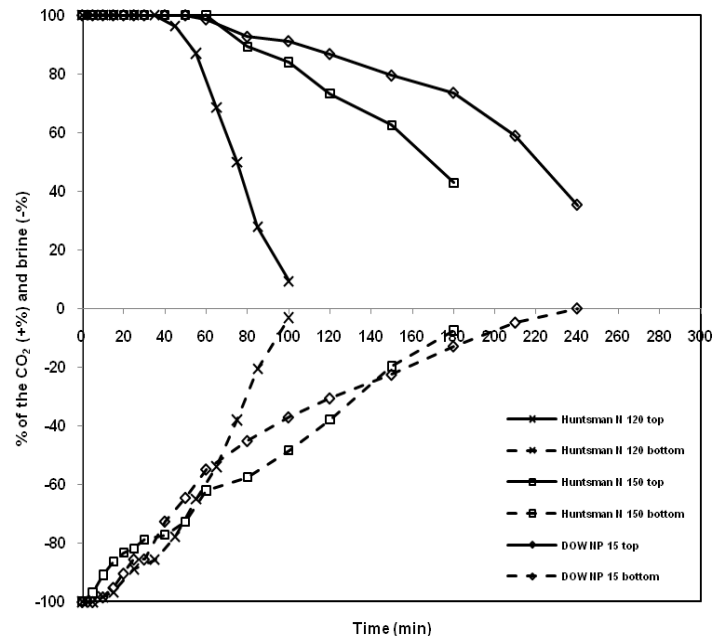


Figure 41: Foam stability of 0.2% Dow NP 15, 0.2% Huntsman N 120, and 0.2 wt% Huntsman N 150 in CO₂ at 3200 psi and 58 °C, with SACROC brine volume ratio 1:1

Other field brines (West Hastings, Delhi, Woodruff, Eutaw) obtained from Denbury Resources were used in foam stability tests at the relevant reservoir conditions using the best foaming agents we have identified. The results show that foams can be stabilized for short periods of time. The results are shown as follows:

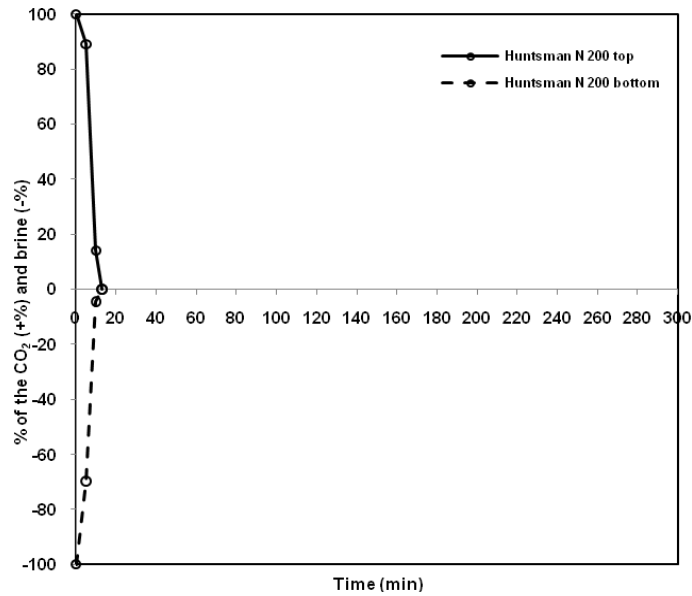


Figure 42. Foam stability of 0.05 wt% Huntsman N 200 in CO₂ at 3150 psi and 71.1 °C, with West Hastings brine (111000ppm) volume ratio 1:1

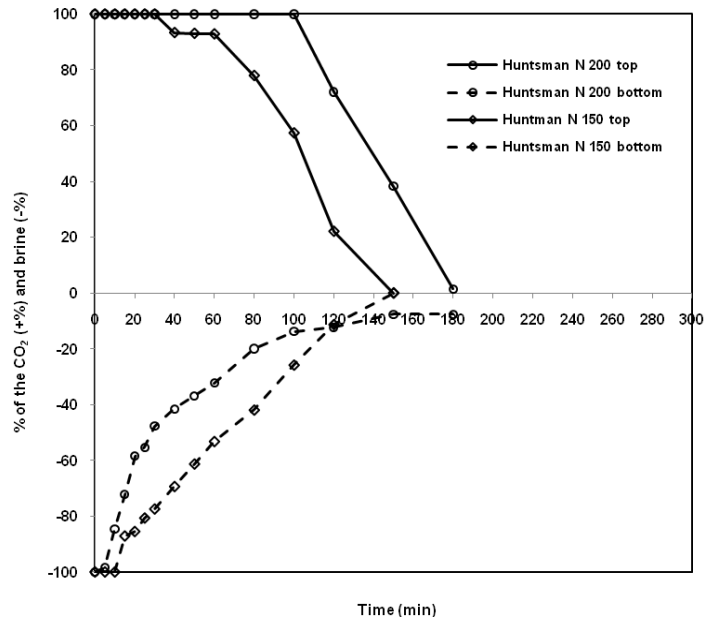


Figure 43. Foam stability of 0.05wt% Huntsman N 150 or 200 in CO₂ at 2100 psi and 57.2 °C, with Delhi brine (78000ppm) volume ratio 1:1

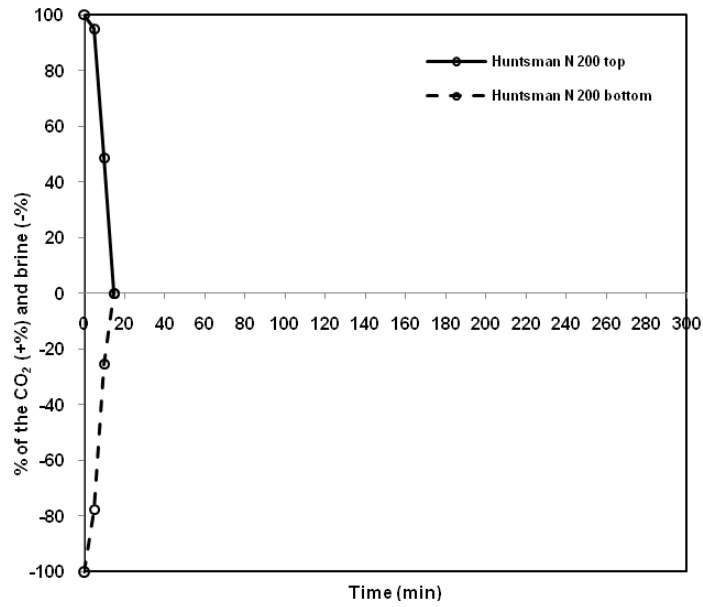


Figure 44. Foam stability of 0.05 wt% Huntsman N 200 in CO₂ at 2600 psi and 73.3 °C, with Woodruff brine (129000ppm) volume ratio 1:1

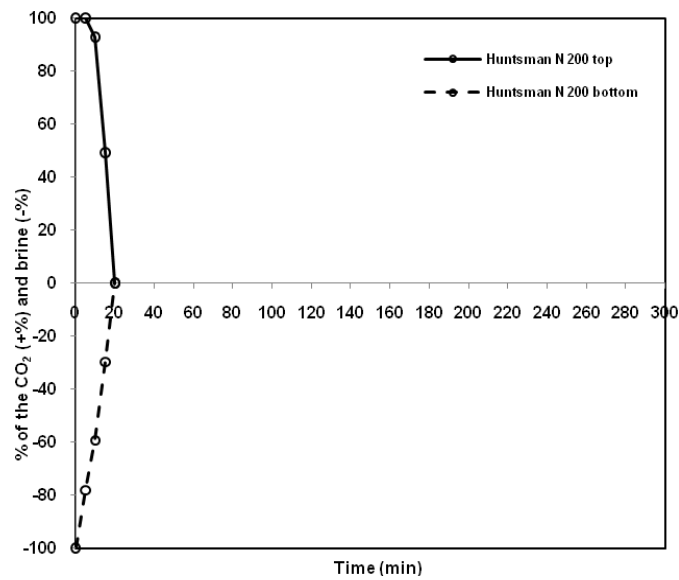


Figure 45. Foam stability of Huntsman N 200 in CO₂ at 2750 psi and 66.7 °C, with Eutaw brine (90000ppm) volume ratio 1:1

5.0 SUMMARY

Two separate projects are discussed in detail in this thesis. Chapter 1 gives a background introduction of CO₂ capture by means of absorption from two classes of CO₂-philic solids: tert-butylated aromatics and sugar acetates. Chapter 2 presents the experiment results of the CO₂ phase behavior of these solid absorbents and techniques used to purify the absorbents. Chapter 3 introduces the background of enhanced oil recovery by CO₂ flooding and the surfactants design guidelines for identifying CO₂ soluble surfactants that may be able to stabilize CO₂-in-brine foams. Chapter 4 presents surfactant solubility and foam stability results at ambient temperature, along with a limited number of results for some of the more promising surfactants conducted with several reservoir brines at reservoir conditions.

In the first project, we were not able to identify any sugar acetate or tert-butylated compound that was capable of melting in the presence of a 1:1 molar mixture of CO₂ and hydrogen at a pressure typical of the post-shift reactor of an IGCC plant. In fact, only one candidate was capable of melting at a pressure less than 10,000 psi (the limit of the equipment); glucose pentaacetate which melted at a pressure of ~6000 psi.

In the second project, several commercially available, inexpensive, low-viscosity, liquid, quick-dissolving, slightly CO₂-soluble, very water-soluble, nonionic surfactants were identified and have promise as CO₂-in-brine foam/emulsion stabilizing agents. The most promising surfactants were, in order of decreasing ability to stabilize a CO₂-in-brine foam, branched alkyl

benzene ethoxylates, linear alkyl benzene ethoxylates, and some of the branched alkyl ethoxylates. None of the linear alkyl ethoxylates were capable of stabilizing a foam. Further, Huntsman N 120, Huntsman 150, and Dow NP 15 were tested with SACROC brine at SACROC reservoir conditions (58 °C, 3200 psi). The foam stability results indicate that these surfactants do have the potential to form foams at reservoir conditions. Future work should include some of the branched alkyl ethoxylates given the environmental concerns associated with the alkyl phenol ethoxylates.

APPENDIX A

VAPOR-LIQUID EQUILIBRIUM FOR H_2+CO_2 SYSTEM

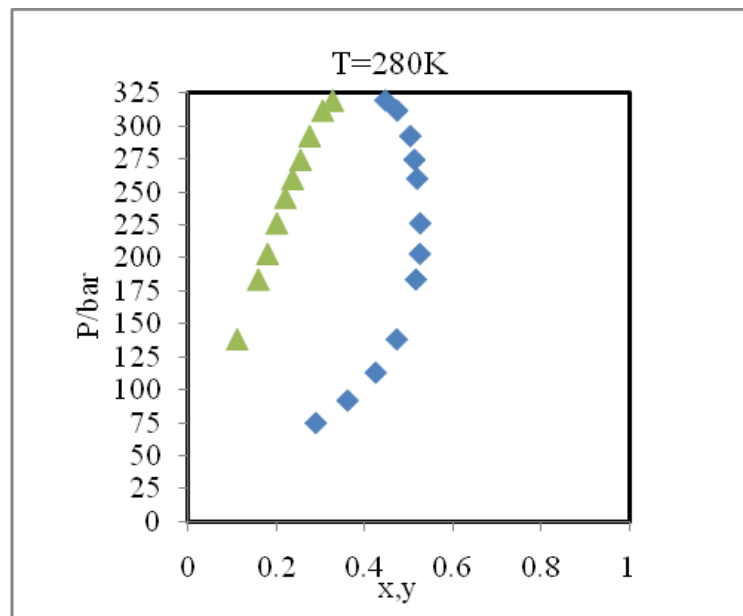


Figure A1: Vapor-liquid equilibrium for H_2+CO_2 binary system at 280 K [5]

▲ x: mole fraction of H_2 in liquid phase, ◆ y: mole fraction of H_2 in gas phase

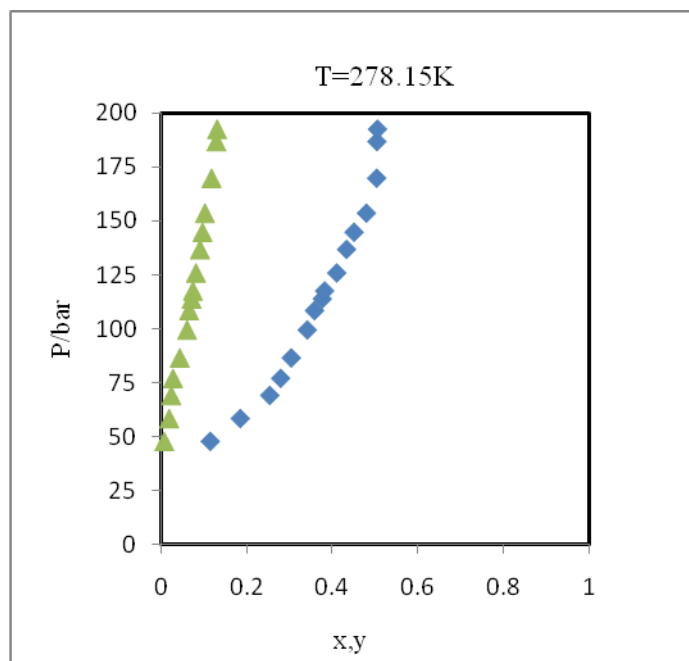


Figure A2: Vapor-liquid equilibrium for H_2+CO_2 binary system at 278.15 K [5]

▲ x :mole fraction of H_2 in liquid phase, ◆ y :mole fraction of H_2 in gas phase

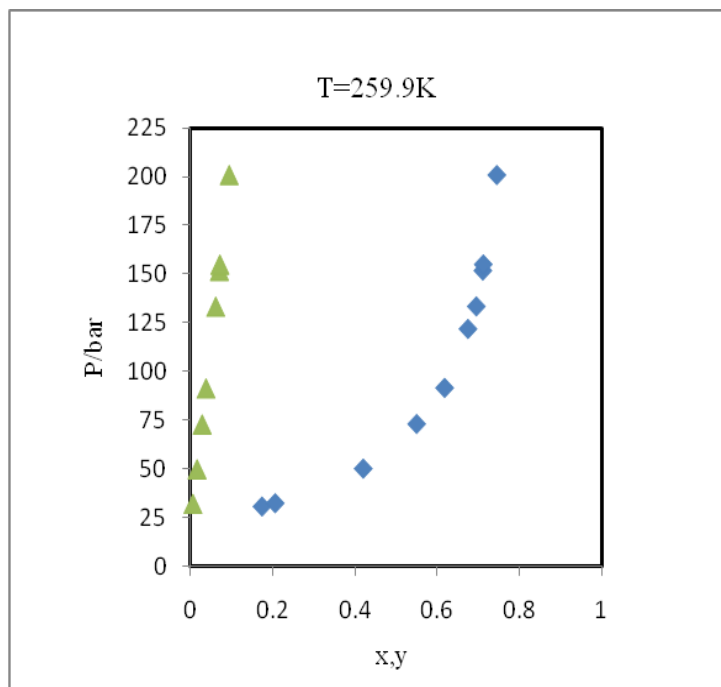


Figure A3: Vapor-liquid equilibrium for H_2+CO_2 binary system at 259.9 K [6]

▲ x :mole fraction of H_2 in liquid phase, ◆ y :mole fraction of H_2 in gas phase

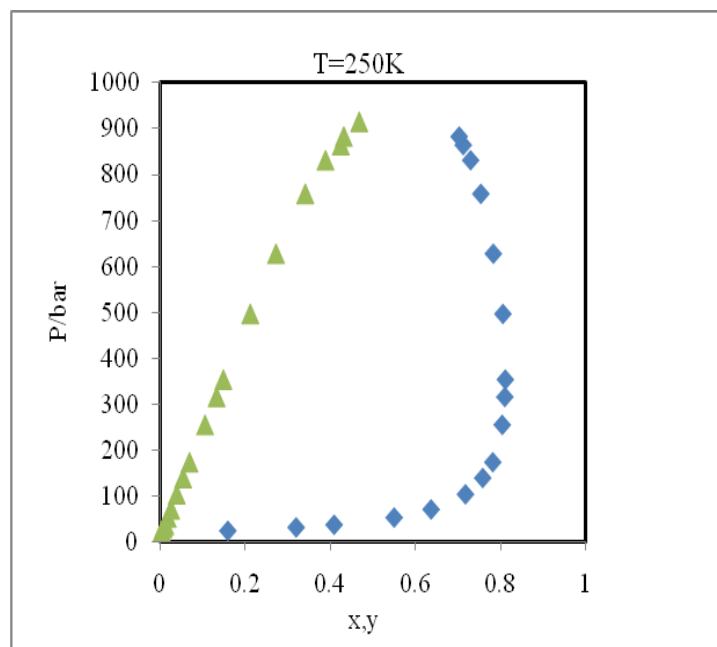


Figure A4: Vapor-liquid equilibrium for H_2+CO_2 binary system at 250 K [7]

▲ x:mole fraction of H_2 in liquid phase, ◆ y:mole fraction of H_2 in gas phase

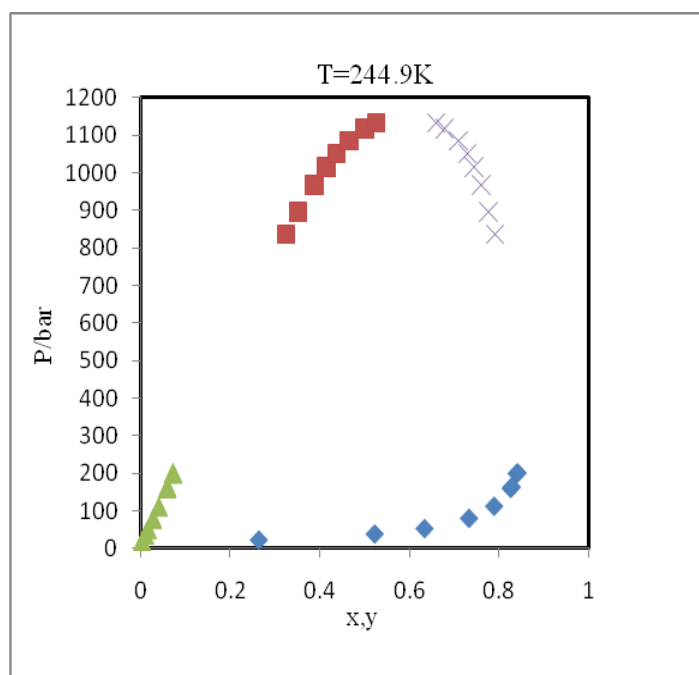


Figure A5: Vapor-liquid equilibrium for H_2+CO_2 binary system at 244.9 K [7]

▲ x:mole fraction of H_2 in liquid phase, ◆ y:mole fraction of H_2 in gas phase

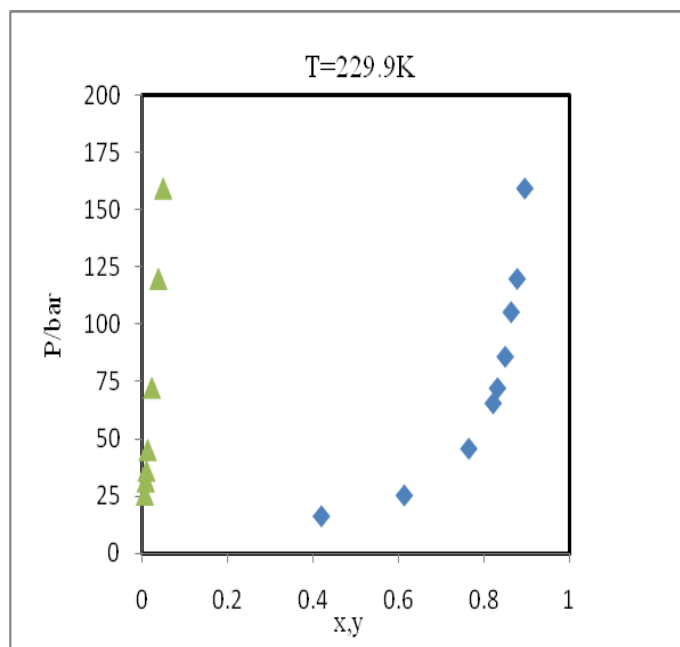


Figure A6: Vapor-liquid equilibrium for H_2+CO_2 binary system at 229.9 K [7]

▲ x :mole fraction of H_2 in liquid phase, ◆ y :mole fraction of H_2 in gas phase

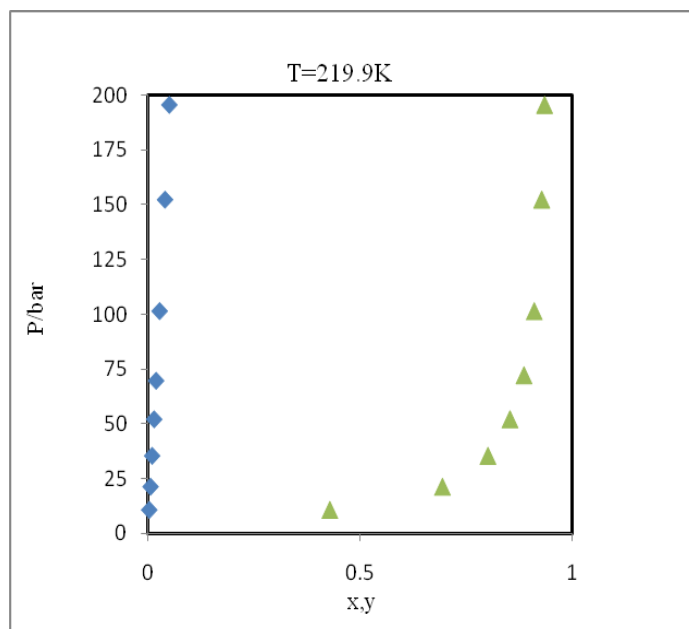


Figure A7: Vapor-liquid equilibrium for H_2+CO_2 binary system at 219.9 K [7]

▲ x :mole fraction of H_2 in liquid phase, ◆ y :mole fraction of H_2 in gas phase

BIBLIOGRAPHY

- 1: L. Hong, E. Fidler, R.M. Enick, R. Marentis, Tri-ter-butylphenol: A Highly CO₂-soluble Sand Binder, *Journal of Supercritical Fluids*.2008,44, pp.1-7
- 2: Hong, L., Thies, M.C., Enick, R.M. Global Phase Behavior for CO₂-philic Solids: The CO₂ + β -D-maltose octaacetate System, *Journal of Supercritical Fluids* 2005,34 (1), pp. 11-16
- 3: Guo, Y., Cao, W. W., Huang, Z.Q. Advances in Integrated Gasification Combined Cycle system with Carbon Capture and Storage technology, 2010 International Conference on Advances in Energy Engineering, ICAEE 2010 , no. 5557541, pp. 363-366
- 4: Carbo, M.C., Boon, J., Jansen, D., van Dijk, H.A.J., Dijkstra, J.W., van den Brink, R.W., Verkooijen, A.H.M. Steam Demand Reduction of Water-gas Shift Reaction in IGCC Power Plants with Pre-combustion CO₂ Capture, *International Journal of Greenhouse Gas Control* 3 (6), pp. 712-719
- 5: K. Bezanehtak, G.B. Combes, F. Dehgani, N.R. Foster, D.L.Tomasko, Vapor-Liquid Equilibrium for Binary Systems of Carbon Dioxide+Methanol, Hydrogen+Methanol, and Hydrogen+Carbon Dioxide at High Pressures, *Journal of Chemical Engineering Data* 2002,47, pp.61-168
- 6: C. Y. Tsang, W. B. Streett, Phase Equilibria in the H₂/CO₂ System at Temperatures From 220 to 290 K and Pressures to 172 MPa, *Chemical Engineering Science*. 1981, 36, pp. 993-1000.
- 7: J. O. Spano, C. K. Heck, Barrick, P. L. Liquid-Vapor Equilibria of the Hydrogen-Carbon Dioxide System, *Journal of Chemical Engineering Data* 1968, 13, pp.168-171.
- 8: Bernard, G., Holm, L., Harvey, C., Use of Surfactant to Reduce CO₂ Mobility in Oil Displacement, *SPE Journal*, 20 (4) 1980, pp.281-292
- 9: Soong, Y., Xing, D., Wei, B., Enick, R.M., Eastoe, J., Mohamed, A., Trickett, K., CO₂-soluble surfactants for enhanced oil recovery mobility control via thickening or in-situ foam generation, *Conference Proceedings, 2009 AIChE Annual Meeting*
- 10: Xu, J., Wlaschin, A., Enick, R.M., Thickening Carbon Dioxide with the Fluoroacrylate-styrene Copolymer, *SPE Journal* 8 (2), pp. 85-91

- 11: Kulkarni, M.M., Rao, D.N., Experimental Investigation of Miscible and Immiscible Water-Alternating-Gas (WAG) Process Performance, Journal of Petroleum Science and Engineering 48 (1-2), pp. 1-20
- 12: Borchardt, J.K., Bright, D.B., Dickson, M.K., Wellington, S.L., Surfactants for Carbon Dioxide Foam Flooding: Effects of Surfactant Chemical Structure on One-Atmosphere Foaming Properties; Chapter 8 of Surfactant-Based Mobility Control: Progress in Miscible Flood Enhanced Oil Recovery; Duane Smith. Editor, ACS Symposium Series 373, Washington, DC, 1988
- 13: Heller, J.; "CO₂ Foams in Enhanced Oil Recovery", Chapter 5 in Foams: Fundamentals and Applications in the Petroleum Industry; Advances in Chemistry Series 242, ACS, Washington DC, 1994
- 14: Heller, J.; Lien, C.; Kuntamukkula, M., Foam like Dispersions for Mobility Control in CO₂ Floods; SPE Journal, 1985, pp.603-613.
- 15: Enick, R.; Holder, G.; Morsi, B.; Thermodynamic Correlation for the Minimum Miscibility Pressure in CO₂ Flooding of Petroleum Reservoirs, February 1988, SPE 14518, SPE Reservoir Engineering, pp.81-92
- 16: Khalil, F.; Asghari, K.; Application of CO₂ Foam As a Means of Reducing CO₂ Mobility, Journal of Canadian petroleum technology, May 2006,45(5), pp. 37-42
- 17: Lee, H.; Heller, J., Laboratory Measurement of CO₂-Foam Mobility, SPE Reservoir Engineering, May 1990, pp.193-197
- 18: Langston, M.V., Hoadley, S.F., Young, D.N., Definitive CO₂ Flooding Response in the SACROC Unit, SPE Reprint Series (51), pp. 34-39